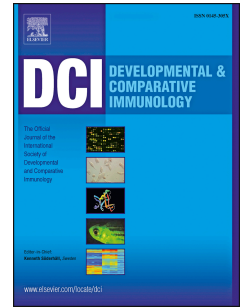


# Accepted Manuscript

Differential expression of novel metabolic and immunological biomarkers in oysters challenged with a virulent strain of OsHV-1

Tim Young, Aditya Kesarcodi-Watson, Andrea C. Alfaro, Fabrice Merien, Thao V. Nguyen, Hannah Mae, Dung V. Le, Silas Villas-Bôas



PII: S0145-305X(16)30481-5

DOI: [10.1016/j.dci.2017.03.025](https://doi.org/10.1016/j.dci.2017.03.025)

Reference: DCI 2858

To appear in: *Developmental and Comparative Immunology*

Received Date: 10 December 2016

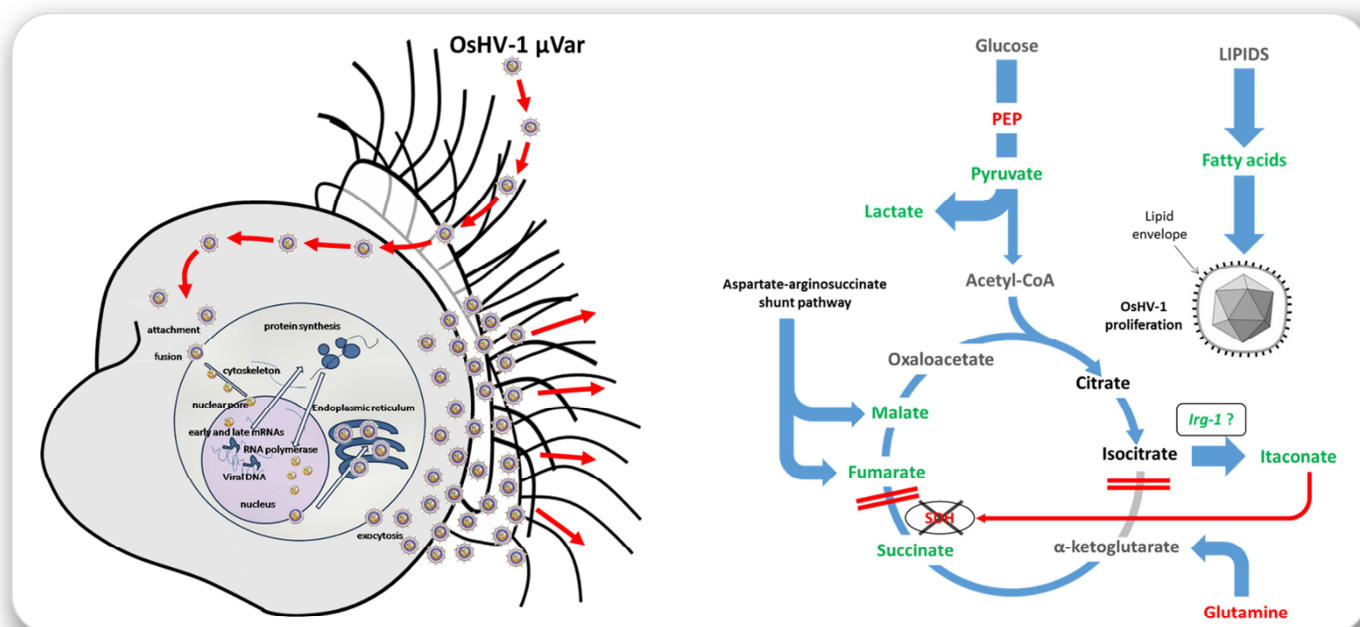
Revised Date: 30 March 2017

Accepted Date: 30 March 2017

Please cite this article as: Young, T., Kesarcodi-Watson, A., Alfaro, A.C., Merien, F., Nguyen, T.V., Mae, H., Le, D.V., Villas-Bôas, S., Differential expression of novel metabolic and immunological biomarkers in oysters challenged with a virulent strain of OsHV-1, *Developmental and Comparative Immunology* (2017), doi: 10.1016/j.dci.2017.03.025.

This is a PDF file of an unedited manuscript that has been accepted for publication. As a service to our customers we are providing this early version of the manuscript. The manuscript will undergo copyediting, typesetting, and review of the resulting proof before it is published in its final form. Please note that during the production process errors may be discovered which could affect the content, and all legal disclaimers that apply to the journal pertain.

## Graphical abstract



**Differential expression of novel metabolic and immunological biomarkers in oysters  
challenged with a virulent strain of OsHV-1**

**Running Head:** Oyster larval immunology

**TIM YOUNG<sup>a,b</sup>**

**ADITYA KESARCODI-WATSON<sup>c</sup>**

**ANDREA C. ALFARO<sup>a</sup>**

**FABRICE MERIEN<sup>d</sup>**

**THAO V. NGUYEN<sup>a</sup>**

**HANNAH MAE<sup>c</sup>**

**DUNG V. LE<sup>a</sup>**

**SILAS VILLAS-BÔAS<sup>b</sup>**

<sup>a</sup>Institute for Applied Ecology New Zealand, School of Science, Faculty of Health and Environmental Sciences, Auckland University of Technology, Private Bag 92006, Auckland 1142, New Zealand

<sup>b</sup>Metabolomics Laboratory, School of Biological Sciences, The University of Auckland, Private Bag 92019 Auckland Mail Centre, Auckland 1142, New Zealand

<sup>c</sup>Cawthron Institute, 98 Halifax Street East, Private Bag 2, Nelson 7042, New Zealand

<sup>d</sup>AUT-Roche Diagnostics Laboratory, School of Science, Faculty of Health and Environmental Sciences, Auckland University of Technology, Private Bag 92006, Auckland 1142, New Zealand

Corresponding author

Andrea C. Alfaro

Phone: +64-9-921-9999 ext. 8197

Fax: +64-9-921-9743

andrea.alfaro@aut.ac.nz

## ABSTRACT

Early lifestages of the Pacific oyster (*Crassostrea gigas*) are highly susceptible to infection by OsHV-1  $\mu$ Var, but little information exists regarding metabolic or pathophysiological responses of larval hosts. Using a metabolomics approach, we identified a range of metabolic and immunological responses in oyster larvae exposed to OsHV-1  $\mu$ Var; some of which have not previously been reported in molluscs. Multivariate analyses of entire metabolite profiles were able to separate infected from non-infected larvae. Correlation analysis revealed the presence of major perturbations in the underlying biochemical networks and secondary pathway analysis of functionally-related metabolites identified a number of prospective pathways differentially regulated in virus-exposed larvae. These results provide new insights into the pathogenic mechanisms of OsHV-1 infection in oyster larvae, which may be applied to develop disease mitigation strategies and/or as new phenotypic information for selective breeding programmes aiming to enhance viral resistance.

**Keywords:** Aquaculture, *Crassostrea gigas*, Larvae, Metabolism, Metabolomics, Ostreid herpesvirus

## 1. INTRODUCTION

With an estimated value of \$4.17 billion USD (FAO 2016), oysters are one of the most commercially important groups of aquatic organisms in the world. In 2014, global aquaculture harvests reached 5.2 million tonnes, representing one third of all cultivated marine molluscs. Although total production volume remains high, growth of the industry has been severely hampered in recent years by extreme disease outbreaks during warmer summer months. Ostreid Herpesvirus (OsHV-1) is a new and emerging viral disease of several molluscan taxa, including oysters (Batista et al. 2015; Sanmartín et al. 2016), scallops (Arzul et al. 2001; Ren et al. 2013), and clams (Xia et al. 2015a; Bai et al. 2016). OsHV-1 has also

been detected in mussels, but without signs of infectivity or adverse consequences (Burge et al. 2011; Domeneghetti et al. 2014), making them a potential reservoir for the virus. Over the past couple of decades, OsHV-1 has been widely associated with mass mortalities of farmed oysters around the globe. A growing number of epidemiology studies and experimental trials suggest that the virus is a causal factor in these events (Friedman et al. 2005; Burge et al. 2007; Segarra et al. 2010; Garcia et al. 2011; Schikorski et al. 2011a,b; Dégremont et al. 2015a,b). With stock losses of up to 100%, economic and social consequences due to the spread of the disease have been devastating in countries such as France, Ireland, USA, China, Australia and New Zealand where oyster aquaculture is a vital primary industry (Burge et al. 2006; Lewis et al. 2012; Castinel et al. 2015). From the perspectives of many scientists, farmers and stakeholders alike, OsHV-1 has been articulated to represent the biggest individual threat to oyster production that the sector has ever faced (Lewis et al. 2012; Castinel et al. 2015).

First evidences for the presence of herpesvirus genetic material in bivalves was obtained in 1976 from samples of *Ostrea edulis* in the UK (Davison et al. 2005). However, widespread detection of herpesviruses and associations with mass mortalities of shellfish were not apparent until the early 1990's (Renault et al. 1995). During the following decade, many occurrences of viral infections were documented around the world, and by 2005 molecular characterisations had led to the designation of the pathogen as the OsHV-1 reference genotype (GenBank accession no. [AY509253.2](#)) (Renault & Arzul 2001; Davison et al. 2005). More recently, there has been an emergence of numerous OsHV-1 variants affiliated with mortalities in different bivalve species displaying different epidemiological characteristics, and it appears that OsHV-1 is undergoing rapid evolution (Grijalva-Chon et al. 2013; Renault et al. 2014; Bai et al. 2015; Martenot et al. 2015). In 2008, the detection of a highly virulent new strain, OsHV-1  $\mu$ Var (GenBank accession no. [HQ842610.1](#)), was

described in association with massive losses of oyster spat in France, Ireland and the UK (Segarra et al. 2010). By 2010, this new variant had reached the coasts of Australia and New Zealand, killing huge numbers of oyster stock within days and leading to sector collapses in certain regions over the following few years (Jenkins 2013; Keeling et al. 2014). Between 2011 and 2013, genetic analysis of cultured oysters from China, Korea and Japan revealed widespread herpesvirus infections from numerous genotypes across the East Asiatic region (Shimahara et al. 2012; Hwang et al. 2013; Jee et al. 2013; Bai et al. 2015, 2016). High mortalities associated with OsHV-1  $\mu$ Var were observed in Swedish and Norwegian hatcheries towards the end of 2014 (Mortensen et al. 2016). More recently, a new outbreak in Tasmania in 2016 has crippled the Australian oyster aquaculture sector and its selective breeding program (Davis 2016; Milne 2016; Whittington et al. 2016). Thus, it is clear that the extent of this new variant's geographical reach is indeed a major global concern.

Due to the widespread prevalence and substantial socioeconomic consequences of OsHV-1  $\mu$ Var, it is vital that knowledge of the interactions between the virus and its hosts are obtained to better understand pathogenesis of the disease, develop mitigation strategies, and guide management decisions. To provide such knowledge, a series of focused research themes relating to the spread of the virus and its mechanisms of infection have been conducted in recent years including genotyping and phylogenetics (Renault et al. 2012; Martenot et al. 2015; Mineur et al. 2015; Burioli et al. 2016), development of experimental infection models (Paul-Pont et al. 2015), modes of transmission (Burge & Friedman 2012; Lionel et al. 2013; Petton et al. 2013; Evans et al. 2016), viral replication and virulence processes (Segarra et al. 2014a, 2016; Green et al. 2015; Martenot et al. 2016), antiviral features of immunity and host responses at transcriptomic and proteomic levels (Renault et al. 2011; Corporeau et al. 2014; Green et al. 2014a,b; Normand et al. 2014; Segarra et al. 2014a,b; He et al. 2015) and identification of virus-resistant traits for selective breeding trials

(Dégremont 2013; Dégremont et al. 2015a,b). Most of these studies have focused on post-metamorphic life stages. However, size and age are significant factors in viral susceptibility and pre-metamorphic larval forms appear to be more vulnerable than their juvenile or adult counterparts (Oden et al. 2011; Dégremont 2013; Paul-Pont et al. 2013; Azéma et al. 2016; Dégremont et al. 2016).

Many oyster farms rely on large-scale hatchery production of larvae to supply spat for growout, with increasing demand and stakeholder interests to enhance larval production capacities (Barnard 2014). Thus, it is essential that we extend our knowledge to characterise the pathophysiology of the disease during early ontogeny. Furthermore, the impacts of OsHV-1  $\mu$ Var on the health of wild populations and their connectivity through larval mortalities, altered larval dispersal potentials, and reduced spat-falls are almost wholly unknown, but are likely to be substantial (Dégremont et al. 2016). In order to assess the ecological consequences of the disease and understand natural vectors and boundaries which may influence its spread, it is important to focus research across all developmental stages. In addition, the identification of specific genotypic and phenotypic traits in larvae which reflect disease susceptibility/resistance would be highly beneficial for monitoring early outcomes of selective breeding programs. Detailed physiological analysis of the host-virus interaction via use of –omics technologies (e.g., transcriptomics, proteomics and metabolomics) may provide fruitful for discovering such traits (Gómez-Chiarri et al. 2015). There are very few studies which have focused on the highly susceptible pre-metamorphic life-stage and, to our knowledge, none which have utilised metabolomic-based approaches to better understand the physiological effect of OsHV-1 infection on homeostatic control mechanisms of metabolism and immunity.

Metabolomics is a newly developing and rapidly advancing field under the –omics banner which aims to provide global snapshots of alterations in the metabolite, or small

molecule (<1 KDa), cellular component (Holmes et al. 2008). Metabolites are the ultimate end-products of gene expression and are strongly influenced by endogenous regulatory mechanisms, as well as by external elements (Fiehn 2002). As intermediates of metabolism, metabolites comprise the available biochemical depot of macromolecular precursors and energy transfer molecules required for optimal organismal growth and functioning. Thus, the composition of the metabolite pool and their flux dynamics provide a closer representation of an organism's phenotype than molecular features at other levels of biological organisation, such as gene transcripts, which may display considerable temporal variations in expression compared to the final phenotypic response, or be entirely decoupled from downstream metabolic processes (Cascante & Marin 2008; Winter & Krömer 2013; Feussner & Polle 2015). With many recent applications across the life sciences (e.g., functional genomics [Sévin et al. 2015], selective breeding [Hill et al. 2015; Hong et al. 2016], aquaculture-related research [Young et al. 2015, 2016; Alfaro & Young 2016], toxicology [Bouhifd et al. 2013; Størseth & Hammer 2014; Chen et al. 2016a] and disease diagnostics, monitoring and prevention [Pallares-Méndez et al. 2016; Wishart 2016]), metabolomics is proving extremely valuable as a highly efficient approach for generating new hypotheses and deciphering complex metabolic and gene regulatory networks of vertebrate and invertebrate models.

By scanning broad sets of metabolic features in whole organisms, tissues or biological fluids in response to environmental influences, such as bacterial or viral infections, metabolomics-based approaches can provide novel information to gain insights into the mechanisms of disease progression, resistance and remediation in aquatic organisms (reviewed by Alfaro & Young 2016; Young & Alfaro 2016). For example, metabolomics has recently been successfully applied to identify biomarkers for *Vibrio* spp. infections in mussels and crabs (Wu et al. 2013; Ellis et al. 2014; Su et al. 2014; Ye et al. 2016), to gain detailed metabolic information on tissue-specific host responses of shrimp and crayfish to white spot



syndrome virus (Liu et al. 2015; Chen et al. 2016b; Fan et al. 2016), and to develop practical treatment methods for streptococcal disease in fish (Ma et al. 2015; Zhao et al. 2015). Although limitedly applied to the investigation of marine invertebrate early life stages thus far, metabolomics has great potential to provide new insights into the interactions between OsHV-1  $\mu$ Var and its oyster larval hosts. Thus, we have conducted the first metabolomics study to assess gross compositional alterations within the oyster larval metabolome in response to OsHV-1 infection.

## 2. METHODS

Refer to the Supplementary Methods file for detailed method descriptors.

### 2.1 Larval challenge

OsHV-1  $\mu$ Var inoculum was prepared from oysters that had been stored at  $-80^{\circ}\text{C}$  and previously tested positive by qPCR (primers: GTCGCATCTTTGGATTAAACAA [BF] and ACTGGGATCCGACTGACAAC [B4], after Martenot et al. [2010]). A whole tissue homogenate was filtered and the virus concentration was determined via qPCR using BF and B4 primers in a SYBR Green assay. Oyster larvae were produced from selectively bred broodstock maintained by the Cawthron Institute (Nelson, New Zealand) and reared in a 170 L conical flowthrough tank to 16 days post-fertilisation, using standard industry protocols. A cohort of healthy larvae was distributed among  $12 \times 2\text{L}$  beakers containing sterile synthetic seawater, at a density of  $7 \text{ larvae mL}^{-1}$ . OsHV-1 inoculum was added to six beakers at a concentration previously determined to cause mortality, with the remaining beakers serving as negative controls (i.e., six replicates per treatment). After 48 hrs, behavioural observations were made and all larvae were snap frozen and stored at  $-80^{\circ}\text{C}$  until metabolite analysis.

## 2.2 Metabolite extraction, analysis and identification

Metabolites were co-extracted with an internal standard using a cold methanol-water method and derivatised via methyl chloroformate (MCF) alkylation according to Villas-Bôas et al. (2011), then analysed via gas chromatography mass spectrometry (Thermo Trace GC Ultra system) according to Smart et al. (2010). Deconvolution of chromatographic data was performed using the Automated Mass Spectral Deconvolution and Identification System (AMDIS v2.66) software. Metabolites were identified using Chemstation software (Agilent Technologies) and customised R xcms-based scripts (Aggio et al. 2011) to interrogate an in-house library of MCF derivatised compounds.

## 2.3 Statistics

Peak intensity data were normalised against the internal standard and by sample-specific biomass, prior to being autoscaled. All statistical analyses were conducted using Metaboanalyst 3.0 (Xia et al. 2015b). Univariate analyses were performed to screen metabolite profile differences between controls and treatments, including foldchange analysis, students *t*-test, Significant Analysis of Metabolites/Microarrays (SAM) and Empirical Bayes Analysis of Metabolites/Microarrays (EBAM). Agglomerative Hierarchical Cluster Analysis (HCA), *k*-means clustering (*k*MC) and Principal Components Analysis (PCA) were used as unsupervised multivariate cluster analyses to identify natural groupings of samples based on the underlying structure of the data. Projection to Latent Structures Discriminant Analysis (PLS-DA) and Random Forrest (RF) analysis were used as supervised multivariate classification analysis methods. The PLS-DA model was validated using Leave One Out Cross Validation (LOOCV), the model performance was assessed via  $R^2$  and  $Q^2$  values, and important classifiers were identified via their Variable Importance in Projection (VIP) scores. RF Receiver Operator Characteristic (ROS) curves were generated by Monte-

Carlo Cross Validation (MCCV) using balanced subsampling. Quantitative Enrichment Analysis (QEA [Xia & Wishart 2010]) and Network Topology Analysis (NTA [Nikiforova & Willmitzer 2007]) were used as pathway analysis methods to investigate functional relationships among the annotated metabolites. Biochemical pathways in the Kyoto Encyclopedia of Genes and Genomes database (Kanehisa & Goto 2000) involving two or more annotated metabolites with simultaneous QEA  $p$ -values  $< 0.05$ , QEA false discovery rates [FDRs]  $< 0.1$ , and with NTA Pathway Impact (PI) scores  $> 0.1$  were considered as potential primary target pathways of interest. Correlation analysis was used to identify major differences in pairwise metabolite correlations (Pearson). Correlation Network Analysis (CNA) was performed to provide enhanced visualisation of metabolite relationships using Cytoscape 3.0 software (Shannon et al. 2003) and the ExpressionCorrelation plugin (Karnovsky et al. 2012).

### 3. RESULTS

The metabolite profiles of oyster larvae exposed to OsHV-1  $\mu$ Var were compared to those from non-exposed control larvae in order to gain insights into the pathogenic mechanisms of infection. Observations of larval behaviour were made every 12 hrs during the trial until first signs of differences between virus-exposed larvae and controls were discerned, i.e., changes in swimming speeds, trajectories and distributions within the water column. After 48 hrs, organisms that had been challenged with OsHV-1  $\mu$ Var tended to be aggregated in the lower 30–50% of the water columns compared to control larvae which were more evenly distributed. When examined under the microscope, virus-exposed larvae also displayed slower motility and abnormal swimming patterns (i.e., horizontal planar circular motions rather than random) characteristic of OsHV-1 infections reported previously (Burge & Friedman 2012; DoA 2015; OIE 2016). However, larval coloration (a commonly used crude

assessment which can indicate severe poor health status) generally appeared to be visually similar between treatments. Mortality assessments revealed that 100% of oyster larvae in all beakers were alive at the time of sampling for metabolomics.

### 3.1 Univariate analysis

GC-MS analysis of larval extracts detected a total of 105 unique metabolites after QC filtering of the data. Of these, 75 were attributed specific chemical identities by matching chromatographic and mass spectral information against our in-house metabolite library (Supplementary Table 1). The remaining 30 features are currently listed as ‘unknowns’ since no matches were found (Supplementary Table 2). Univariate statistical analyses showed a number of differences in the metabolite profiles between control and virus-infected larvae (Figure 1). SAM identified 30 metabolites as being differentially ( $p < 0.05$ ) expressed between larvae exposed to OsHV-1  $\mu$ Var and control larvae with an FDR of 3.1% (Figure 1A), whereas EBAM identified 28 metabolites as being differentially expressed with an FDR of 4.7% (Figure 1B). The summarised results of student’s  $t$ -test, SAM and EBAM are displayed in Figure 1C, along with their relative fold changes. Taking the results of these analyses together, the abundances of nine metabolites were likely under expressed in virus-infected larvae compared to the metabolic baseline of control organisms, and 20 metabolites were likely over expressed. Full details of the univariate statistical analyses are provided in Supplementary Tables 1 and 2.

### 3.2 Unsupervised multivariate cluster analysis

Unsupervised multivariate analyses of entire metabolite profiles revealed that good separation between control and virus-infected larvae could be obtained based on the underlying structure of the data (Figure 2). HCA correctly positioned samples into two main groups (group 1, controls  $n = 6$ ; group 2, treatment  $n = 6$ ) (Figure 2A), indicating that the

within-class variation was considerably lower than the between-class variation. *k*MC corroborated this by also correctly assigning larval samples into groups based on the treatment that they received (Figure 2B; inserted table). PCA produced a 2-D score plot containing two distinct clusters of samples which appropriately reflected their class labels and with no indication of sample outliers (Figure 2C). The two clusters are separated along PC1 with the relative abundances of around 40 metabolites explaining much of the divide (see Supplementary Tables 1 and 2 for the PCA loadings). Although the calculated 95% confidence interval ellipses overlapped, the accumulative variation among all samples explained by PC1 and PC2 was only 46.0%. It is therefore possible that the OsHV-1  $\mu$ Var-infected larval samples may be separated from control samples along other PC vectors not discernible in the 2-D score plot which might be revealed via supervised multivariate techniques.

### 3.3 Supervised multivariate classification analysis

Supervised multivariate classification analysis was clearly able to discriminate larval samples based on the treatment they received (Figure 3). Compared to PCA, the 2-D PLS-DA score plot better separated virus-infected from control larval samples along the x-axis (Figure 3A), with good cross-validated model performance using the first two latent variables (Accuracy = 100%;  $R^2 = 96.9\%$ ;  $Q^2 = 79.6\%$ ) (Figure 3B). PLS-DA additionally informed upon which metabolites were most important for the classification model via their VIP scores (Figure 3C). Significant classifiers for the separation between virus-infected and control groups were ranked, yielding 43 metabolites (35 annotated and 8 unannotated) with VIP scores  $> 1.0$  (Figure 3C and Supplementary Tables 1 and 2). In addition to the 30 differing metabolite abundances identified via SAM and/or EBAM (Figure 1C), PLS-DA also

recognised 2-aminobutyric acid, glycine, hexanoic acid, homocysteine, putrescine, valine, and four additional unannotated metabolites as being important classifiers.

The RF machine learning algorithm was further employed as a complimentary feature selection method to similarly rank the most salient metabolite features responsible for class separation via a different statistical approach more resistant to over fitting than PLS-DA (Figure 4). A default RF classification model was first constructed using ten features (i.e.,  $\sim \sqrt{n}$ ) and 500 permutations, which correctly classified all samples. A series of ROC curve analyses were then performed to generate various  $n$ -feature classification models which were validated using MCCV sub-sampling to assess predictive accuracies (Figure 4A). The predictive accuracies of the 5-, 10-, and 15-feature RF models were 94.5, 98.0, and 100%, respectively, with AUC's of 0.985, 1.0, and 1.0, respectively (Figure 4B). ROC curve analysis of the 5-feature model with corresponding confidence intervals is shown in Figure 4C, and the predicted class probabilities of the model is shown in Figure 4D. The average importance and selected frequencies of metabolites in the 5-feature RF model are shown in Figure 4E and Figure 4F, respectively. Most metabolites identified as potential biomarker candidates via SAM, EBAM and PLS-DA were also selected to some degree by RF which further corroborates their significance as key classifiers of larval health condition. The most frequently selected compounds (> 20%) with high measures of average importance (> 1.0) were fumaric acid, 4-hydroxyphenylacetic acid, glutamine, glutaric acid, myristic acid, 2-aminoadipic acid, and two unannotated metabolites. As indicated by RF, a low error of classification could be obtained with few compounds.

### 3.4 Functional biochemical pathway analysis

Based on the profiles of annotated metabolites, metabolic pathway analyses were performed to reveal the most relevant pathways related to the pathophysiology of oyster larvae exposed

to OsHV-1  $\mu$ Var (Figure 5) (see Supplementary Table 3 for full analysis details). A total of 43 biochemical pathways were recognised from within the KEGG database which contained one or more of the annotated metabolites detected. Pathways involving two or more detected metabolites and with simultaneous QEA  $p$ -values  $< 0.05$ , QEA FDR values  $< 0.1$ , and NTA Pathway Impact (PI) values  $> 0.1$  were screened as potential primary target pathways of interest relating to the treatment effect. According to these selection criteria, 12 biochemical pathways were identified with evidence of metabolic disturbances in virus-exposed larvae (Figure 5A), comprising of: glycolysis/gluconeogenesis; pyruvate metabolism; tricarboxylic acid cycle; glyoxylate and dicarboxylate metabolism; aminoacyl-tRNA biosynthesis; tyrosine metabolism; alanine, aspartate and glutamate metabolism; arginine and proline metabolism; glycine, serine and threonine metabolism; cysteine and methionine metabolism; D-glutamine and D-glutamate metabolism; and nicotinate and nicotinamide metabolism. Nine further pathways that were identified statistically via QEA ( $p < 0.05$ ) but did not meet one or more of our other ideal impact assessment criteria were screened as potential secondary target pathways of interest, comprising of: purine metabolism; pyrimidine metabolism; tryptophan metabolism, lysine degradation; nitrogen metabolism; fatty acid biosynthesis; fatty acid elongation in mitochondria; biosynthesis of unsaturated fatty acids, and fatty acid metabolism.

### 3.5 Correlation analysis

Pairwise metabolite–metabolite correlation matrices of Pearson coefficients for each treatment group were separately constructed and displayed as heatmaps (Figure 6). In general, substantial treatment-induced differences in the relationships between metabolites were exposed, as demonstrated by the many contrasting colours of same cells between the two heatmaps. From these totals of 5565 pairwise comparisons within each dataset, 167 strong

linear correlations ( $R^2$  values  $> 0.7$  or  $< -0.7$ ) were found to be highly differentially expressed (i.e., positive vs negative relationships) between larvae infected with OshV-1  $\mu$ Var and baseline controls. Correlation network analyses (CNA) with selection criteria of  $R^2 > 0.9$  or  $< -0.9$  were then separately performed on control and virus-exposed larval datasets to summarise and reveal the major correlation differences in the metabolic networks (Figure 7).

#### 4. DISCUSSION

The aim of this study was to evaluate changes in the *C. gigas* oyster larval metabolome induced by ostreid herpesvirus and determine whether metabolomics-based approaches can deliver novel mechanistic insights into immunological defence systems of early life-stage marine invertebrates. Thus, we performed a comprehensive determination of metabolic alterations in oyster larvae exposed to the newly emerging and highly virulent OshV-1  $\mu$ Var genotype via GC/MS-based metabolomics. Our findings revealed that viral exposure had an effect on many metabolites involved in central carbon metabolism, across broad chemical classes with various functional roles. These virus-induced changes in the metabolite profiles enabled us to discriminate healthy from unhealthy larvae via multivariate clustering and classification techniques, discern relationships among metabolites, identify entire biochemical pathways evidenced of being altered, and further focused our attention towards specific mechanisms of immunity characteristic of the pathophysiological condition. We identified coordinated changes in tricarboxylic acid (TCA) cycle-related metabolites in virus-exposed larvae indicative of abnormal energy metabolism and biosynthesis of an antimicrobial product, and also detected subtle signs of potential oxidative stress, transformation or degradation of extracellular matrix scaffolding, and disruption of normal lipid metabolism suggestive of requirements for viral appropriation of host-cell biomaterial, among other processes. Confirmation of these hypotheses based on the metabolomics data



will require further investigation using functional assays at other levels of biological organisation.

#### 4.1 Lipid metabolism

Enveloped viruses, such as those from the herpesviridae family, are known to physically and metabolically remodel host cells during infection to create optimal environments for their replication by manipulating lipid signalling and metabolism (Chukkapalli et al. 2012; Rosenwasser et al. 2016). Such viruses instructively alter host metabolism in order to supply the high quantities of fatty acids which are required as vital lipid envelope components during virion assembly (Koyuncu et al. 2013). Although the precise induction mechanisms have not yet been elucidated, enrichment of host fatty acid (FA) production is a common response of different organisms to infection by various enveloped viruses (Mazzon & Mercer 2014; Hsieh et al. 2015; Sanchez & Lagunoff 2015), including herpes-type viruses such as human cytomegalovirus (HCMV) (Spencer et al. 2011; Seo et al. 2013; Purdy et al. 2015) and Kaposi's sarcoma-associated herpesvirus (Bhatt et al. 2012). An emerging theme is that these lipid-modifying pathways are linked to innate antiviral responses which can be modulated to inhibit viral replication (Chukkapalli et al. 2012). For example, HCMV stimulates free fatty acid (FFA) production to enable and enhance assembly of infectious virions by activating expression of *ACCI* host mRNA, the gene encoding for the rate-limiting enzyme acetyl-CoA carboxylase (ACC) involved in the initial commitment stage of *de novo* FA synthesis (Spencer et al. 2011); whereas pharmacological inhibition of host ACC substantially limits the ability of HCMV to replicate (Munger et al. 2008). More recently, Koyuncu et al. (2013) reported that siRNA-induced knockdown of a suite of other enzymes involved in FA synthesis (fatty acyl-CoA synthetases and elongases) inhibited herpesvirus replications, whereas knockdown of proteins responsible for FA catabolism (the peroxisomal  $\beta$ -oxidation

enzyme acetyl-CoA acyl-transferase 1) and the first step of triglyceride synthesis (1-acylglycerol-3-phosphate O-acyltransferase 9) enhanced viral replication by elevating the available FFA pool. Thus, the FA synthesis pathway is currently gaining considerable attention as a prime target for the development of innovative therapeutics that are not dependent on mechanisms of adaptive immunity, and therefore resilient to emerging virus variants which have become resistant to anti-viral therapies (Goodwin et al. 2015).

Looking at the global metabolic changes in larvae induced by OsHV-1  $\mu$ Var exposure, there was a signature consisting of FFAs, presumably involving either a change in the relative rates of production and/or breakdown. These variation patterns contributed towards earmarking FA pathways (FA metabolism, FA  $\beta$ -oxidation and FA elongation in mitochondria) as being candidate targets of interest in our study via secondary bioinformatics techniques, and also were key metabolites causative to the perturbations observed within the differential metabolic correlation networks. Under the starvation conditions we employed during the viral challenge, an effect on basal lipolysis would be the most obvious potential mechanism for the FFA changes observed here. Compared to non-infected control larvae, the general increase in medium and long chain FFAs (C16:0, C18:3n-6, C20:4n-6, C20:5n-3, C22:2n6, C22:6n-3) and microalgal-derived dietary FFAs (C14:0, C16:1n-7) in virus-infected larvae are indicative of enhanced catabolism of endogenous triacylglycerol lipid supplies. This pre-metamorphic host-response appears to be somewhat similar to that of post-metamorphic life stages. Proteomic-based analyses of adult Pacific oysters experimentally infected with OsHV-1  $\mu$ Var recently identified that a key enzyme involved in the first step of lipid hydrolysis, triacylglycerol lipase (TGL), was over-accumulated in virus-exposed animals which likely reflects enhanced lipolysis during initial stages of infection (Corporeau et al. 2014). Furthermore, transcriptomic-based analyses revealed over-expression of genes encoding for TGL and phospholipase A2 (an enzyme that releases FAs from the second

carbon group of glycerol in phospholipids) in OsHV-1  $\mu$ Var-infected oysters (He et al. 2015), and several other studies also report triglyceride levels being substantially decreased in juvenile and adult oyster hosts exposed to the virus (Pernet et al. 2010, 2014; Tamayo et al. 2014). In adult oysters, FFA accumulations do not appear to coincide with the reduced lipid contents following OsHV-1  $\mu$ Var infection likely due to them being transitory intermediates (Tamayo et al. 2014), for which simultaneously enhanced rates of  $\beta$ -oxidation could explain. However, infected adult oysters display a down-accumulation in fatty acid-binding protein (FABP) (Corporeau et al. 2014), a chaperone involved in trafficking FFAs across the mitochondrial membrane, and, at the height of the viral load, decreased *Fabp* transcription and expression of a gene encoding the alpha subunit of FA oxidation complex (He et al. 2015), all of which would limit  $\beta$ -oxidation rather than promote it. Thus, aside from being used for host energy metabolism, the FFAs produced during virus-induced lipolysis in oysters may be used as precursor synthesis molecules for constructing the lipid envelope during virus assembly and proliferation; as previously reported for HCMV infections.

Although FFA levels at a particular time reflect the complex metabolic balance between lipolysis,  $\beta$ -oxidation, and any other FA production (e.g., *de novo* synthesis) or consuming processes (e.g., triglyceride synthesis and utilisation for virion assembly), the FFA accumulations we observed are consistent with the general findings of other studies which have investigated various models of herpes-type infections. Perhaps a key point of difference in host-virus interactions between OsHV-1 and vertebrate-infecting herpesviruses could be the primary source from which the FAs are derived from (i.e., lipolysis vs *de novo* synthesis). We recommend that targeted analyses of these pathways are additionally conducted at transcriptional and translational levels, in combination with metabolite profiling, in order to tease out the mechanistic intricacies of OsHV-1  $\mu$ Var-induced modulation of host lipid metabolism in oyster larvae. With FAs being necessary components required for OsHV-

1 replication and proliferation, establishing the precise viral targets of host lipid metabolism could assist in the development of antiviral therapeutics, and/or identification of unique disease resistant genomic or metabolic traits for selective breeding purposes.

## 4.2 TCA cycle and immunoresponsive gene 1

Host metabolism changes are suggestive of immunoresponsive gene 1 (*Irg1*) like activation, which directly affects carbon flux through the TCA cycle and modifies energy metabolism. *Irg1* is commonly and highly expressed in vertebrate macrophages during inflammation and infection by a variety of pathogens (Preusse et al. 2013). *Irg1* encodes immune-responsive gene 1 protein/ *cis*-aconitic acid decarboxylase (IRG1/CAD) which links cellular metabolism with immune defence by catalysing the decarboxylation of *cis*-aconitic acid (the citrate → isocitrate isomerisation intermediate in the TCA cycle) to itaconic acid (ITA) (Michelucci et al. 2013; Vuoristo et al. 2015). ITA is a metabolite with potent antimicrobial properties (Naujoks et al. 2016), and was identified in our study as being over-accumulated in virus-exposed oyster larvae. ITA being discovered as the gene product of *Irg1* is arguably one of the most important biological insights made in recent times (Sévin et al. 2015), and was only revealed through taking a non-hypothesis driven metabolomics profiling approach as we have in the current study. ITA has newly been recognised as a crucial regulatory metabolite involved in posttranscriptional mechanisms of reprogramming mitochondrial metabolism through modulation of substrate level phosphorylation, TCA cycle flux and succinic acid signalling (Mills & O'Neill 2016; Cordes et al. 2016; Németh et al. 2016), production of inflammatory cytokines (Lampropoulou et al. 2016) and its ability to alter cellular redox balance (Tretter et al. 2016).

Upregulation of *Irg1* transcription leads to a characteristic metabolic signature of a “broken TCA cycle” in stimulated macrophages (O'Neill 2015; O'Neill & Pearce 2016;

O'Neill et al. 2016). ITA accumulation represents the first of two distinctive break-points in the pathway due to decreased transcription of isocitrate dehydrogenase (IDH; catalyses isocitrate  $\rightarrow$   $\alpha$ -ketoglutarate), and the redirection of *cis*-aconitic acid metabolism via enriched *Irg1*-encoded IRG1/CAD expression (Jha et al. 2015; Yanamoto et al. 2015). The increased production of ITA decreases citric acid oxidation through the cycle. To compensate for the reduced flux under such conditions, Maisser et al. (2016) showed that glutamine uptake is co-enhanced with *Irg1* expression, serving to replenish the pathway with  $\alpha$ -ketoglutaric acid through glutaminolysis. In agreement, the reduction in free glutamine content that we observed in OsHV-1  $\mu$ Var-exposed larvae is consistent with such an anaplerotic mechanism. Herpes-infected human cells can switch substrate utilisation from glucose to glutamine to accommodate the biosynthetic and energetic needs of the viral infection, and allow glucose to alternatively be used biosynthetically (Chambers et al. 2010). Virus-induced reprogramming of glutamine metabolism and anaplerosis of the TCA cycle at this particular point appears to be critical for successful replication of herpes-type viruses, as well as maintenance of cellular viability during latent infections (Sanchez et al. 2015; Thai et al. 2015).

The second characteristic break-point in the TCA cycle occurs at succinate dehydrogenase/ respiratory Complex II (SDH/CII), the enzyme which catalyses the oxidation of succinate  $\rightarrow$  fumarate, and also crucially regulates respiration in the electron transport chain (Mills & O'Neill 2016). ITA is a competitive inhibitor of SDH/CII (Cordes et al. 2016), and thus, when ITA levels increase, enzyme activity is attenuated leading to an accumulation of succinic acid and a concomitant decrease in oxidative phosphorylation (OxPhos) (Lampropoulou et al. 2016). Directly in line with this second TCA cycle break-point feature, oyster larvae exposed to OsHV-1  $\mu$ Var exhibited elevated levels of succinic acid. The functional purpose of reprogramming host cell metabolism to accumulate succinic acid in response to pathogen infections appears to stem in part from its ability to mediate

inflammatory responses. Aside from having a fundamental role in the TCA cycle, succinic acid can act as a regulatory signal, via succinate receptor 1 (GPR91/SUCNR1), to induce production of pro-inflammatory cytokines (TNF- $\alpha$ , IL-1 $\beta$ ) which can enhance immune-stimulatory capacity, but also can exasperate disease when produced in excess (Rubic et al. 2008; Tannahill et al. 2013; Mills & O'Neill 2014; Littlewood-Evans et al. 2016). GPR91/SUCNR1 is therefore involved in sensing the immunological danger exposed by *Irg1*/ITA-induced succinic acid accumulations, thus further establishing direct links between immunity and cellular respiration.

Rather than downstream TCA cycle intermediates being depleted as a consequence of this second break at SDH/CII, the metabolic response involves enrichment of the aspartate-arginosuccinate shunt pathway which provides a compensatory mechanism to replenish the system (Jha et al. 2015), thus leading to significant increases in levels of fumaric and malic acids regardless of SDH/CII inhibition (Lampropoulou et al. 2016). In agreement, both of these TCA metabolites were over-accumulated in virus-exposed larvae. Thus, our metabolite data suggest that larval oyster cells have a comparable host response to OsHV-1  $\mu$ Var as mammalian macrophages when stimulated or infected with other viruses. To the best of our knowledge, this is the first report of such metabolic reprogramming of the TCA cycle in an invertebrate with the specific metabolite signature of pathogen-induced *Irg1* transcription directly in accordance with vertebrate cell models. How OsHV-1 might stimulate genomic components leading to activation of *Irg1* transcription in oysters is not known, but would likely share some parallels with mechanisms of higher taxa (see Owens & Malham 2015; Naujoks et al. 2016; Tallam et al. 2016).

Only two cases of *Irg1* involvement in marine mollusc immune responses have thus far been reported. Martín-Gómez et al. (2012) detected an up-regulation of *Irg1* transcription in the flat oyster, *Ostrea edulis*, exposed to Bonamiosis disease under light and

heavy infection scenarios, which suggest that *Irg1* could play a role at early infection stages with prolonged expression at later stages. Furthermore, although not stated nor discussed in their manuscript, He et al. (2015 [supplementary material]) identified via untargeted gene expression profiling that the *C. gigas Irg1* transcript was over-expressed 9-fold in adult oysters exposed to OsHV-1 at the height of the viral replication process. In combination with our findings of a classic metabolic signature for *Irg1* over-expression and enhanced aconitase activity in virus-exposed larvae, these data are supportive of an active role of *Irg1* and its metabolic product, ITA, in the innate immunity of oysters, and further provide the first reports of such associated pathophysiological mechanisms of disease in marine invertebrates. Moreover, these data also suggest that this particular metabolic reprogramming mechanism develops very early in the oyster lifecycle, and is a conserved feature of immunity across the metamorphic boundary. These findings provide fresh insights into the early evolution of innate immunity. We suggest that a detailed characterisation of this system, including endogenous regulatory networks and exogenous effectors, be conducted through ontogeny which may provide useful information for identifying disease resistant traits. Investigation of other mechanisms associated with altered host energy metabolism, such as the Warburg effect, may also deliver important insights into the pathophysiology of the disease.

#### **4.3 Warburg effect**

The Warburg effect is an abnormal metabolic shift that was first discovered in proliferating cancer cells (Ferreira 2010). It has since been detected in vertebrate cells infected by viruses (Delgado et al. 2010, 2012; Darekar et al. 2012; Thai et al. 2014), and was recently implicated as an actuated pathway during viral infections in shrimp and oysters (Corporeau et al. 2014; Su et al. 2014; Hsieh et al. 2015; Fan et al. 2016; Li et al. 2016). Herpes-type viruses are known to activate oncogenes, thus providing a mechanistic link with cancerous



cell phenotypes (Mesri et al. 2014). The Warburg effect is distinguished by a high rate of glycolytic flux and unusual aerobic fermentation of glucose to lactic acid even though there is enough oxygen available for OxPhos to proceed (Kelly & O'Neill 2015). It is often accompanied by the activation or enrichment of other metabolic pathways that provide energy and direct the flow of carbon and nitrogen, such as the pentose phosphate pathway, nucleotide biosynthesis, lipolysis, and glutaminolysis (Zaidi et al. 2013; Tannahill et al. 2013; Su et al. 2014; Sanchez & Lagunoff 2015; Li et al. 2016), and also with mechanisms of innate immunity such as *Irg1* activation/ ITA over-accumulation (Kelly & O'Neill 2015).

Metabolic alterations characteristic of the Warburg effect involves increased glycolysis, elevated levels of lactic acid, and changes in rates of nicotinamide adenine dinucleotide phosphate (NADPH) production/utilisation. These effects result from the diversion of glucose metabolism, glutamine oxidation, and requirements of reducing equivalents for FA biosynthesis and for mounting anti-oxidant responses to Reactive Oxygen Species (ROS) via re-oxidisation of glutathione (vander Heiden et al. 2009; Weljie & Jirik 2011; Senyilmaz & Teleman 2015). Although the precise initiating mechanism/s responsible for reprogramming the glycolytic and gluconeogenic pathways that result in these metabolite changes are not yet completely understood (Vijayakumar et al. 2015), succinic acid accumulations act as an innate immunity regulatory signal to trigger a switch in core metabolism from OxPhos to glycolysis. Succinic acid stabilises the alpha subunit of hypoxia inducible factor 1 (HIF-1 $\alpha$ ) thereby activating transcription of genes which downregulates OxPhos (e.g., via indirect inhibition of pyruvate kinase to reduce TCA cycle flux), enhances glycolysis (e.g., via increased production of hexokinase and glucose transporters), and promotes lactic acid production (e.g., via regulation of lactate dehydrogenase and monocarboxylate transporter 4) (Ben-Shlomo et al. 1997; Selak et al. 2005; Semenza 2010; Palsson-McDemott & O'Neill 2013; Tannahill et al. 2013; Mills & O'Neill 2014). Thus, with



ITA-induced inhibition of SDH/CII, succinic acid may be an important metabolite linking *Irg1* activation with the Warburg effect in virus infected cells.

Compared to baseline control larvae, lactic acid was over-accumulated in OsHV-1  $\mu$ Var-exposed larvae, whereas NADPH levels were lower. Secondary bioinformatics analysis of the metabolomics data also recognised glycolysis/gluconeogenesis and nucleotide metabolism as being differentially modulated as a larval host response to the virus, which could reflect an active Warburg-like effect. Our findings align with those of Corporeau et al. (2014) who utilised a proteomic-based approach to assess global protein changes in adult oysters infected with OsHV-1  $\mu$ Var. Altered host protein expressions included changes in mitochondrial membrane permeability (accumulation of voltage-dependant anion channels [VDAC]), and enhanced glycolysis via an increase in the glycolytic enzyme Triose phosphate isomerase and decreases in the gluconeogenic enzymes Fructose 1,6-biphosphatase and Malate dehydrogenase (MDH); signatures which resemble induction of the Warburg effect (Chen et al. 2011; Maldonado & Lemasters 2012; Corporeau et al. 2014). Supporting the findings of Corporeau et al. (2014), increased and decreased expressions of genes encoding VDAC and MDH, respectively, were detected in adult oysters exposed to the virus (Renault et al. 2011; He et al. 2015). Taken together, these characteristic evidences at various levels of organisation (i.e., gene, protein and metabolite) suggest an involvement of the Warburg effect as a pathophysiological feature of OsHV-1  $\mu$ Var infection.

It is thought that the Warburg effect in cancer cells is adapted to facilitate the uptake and incorporation of nutrients into the biomass needed to produce new cells during proliferation at the expense of efficient, albeit slow, ATP production via OxPhos (vander Heiden et al. 2009; Zhang et al. 2012). The functional purpose for selection of energy inefficient lactic acid fermentation over OxPhos in virus-exposed oysters is less clear. However, it is possible that the Warburg effect is ‘strategically’ induced by OsHV-1 as a

metabolic reprogramming mechanism beneficial to the pathogen. With the catabolism of glucose exceeding the bioenergetics needs of cells during Warburg activation (Thomas 2014), the high yields of intermediates created through enriched glycolysis and a truncated TCA cycle could be used for production of purine and pyrimidine nucleotides and other components required for viral DNA synthesis and envelope assembly. Aerobic fermentation would also provide energy for these processes more swiftly than through OxPhos and with less risk of constraining glycolytic flux via ATP-induced negative feedback inhibition (Zhang et al. 2012; Sanchez & Lagunoff 2015), thus facilitating rapid and persistent viral replication.

#### 4.4 Oxidative stress

We hypothesised that significant changes in the abundances of metabolites reflective of oxidative stress would be represented in OsHV-1 Var-exposed oyster larvae. Exposure to invading pathogens initially triggers robust innate immune responses, and a rapid release of reactive oxygen species (ROS) called an oxidative burst is usually registered soon afterwards (Torres et al. 2006). ROS are beneficial since they can facilitate degradation of invading pathogen biomaterial, and also act as signalling molecules to potentiate other immune responses, such as activation of interferons and their regulatory factors (Chiang et al. 2006). However, when produced in excess, they can cause irreparable damage to crucial host cells through degradation of macromolecular cellular components, including lipids, proteins, and DNA (Pisoschi & Pop 2015). During viral infections, this can actually promote virus proliferation by enhancing dispersion from lysed or apoptotic cells (Stehbens 2004). Thus, oxidative bursts should ideally be reduced before attaining critical levels, and can be achieved through an intricate balance of co-regulated antioxidant processes. These include production of the antioxidant metabolite glutathione (GSH) and a number of enzymes which regulate GSH turnover, directly recycles ROS, or are involved in repairing ROS-induced damage

(Knight 2000; Apel & Hirt 2004). Adult and juvenile oysters exposed to OsHV-1, or showing variable susceptibilities to disease associated with the virus, display differential expression of these enzymes, and/or the genes which encode them (Fleury et al. 2010; Fleury & Huvet 2012; Schmitt et al. 2013; Normand et al. 2014; Corporeau et al. 2014; He et al. 2015). This indicates a change in ROS balance and induction of oxidative stress as a response to the infection, and also suggests that the ROS-regulatory system is an important feature which underpins disease resistance.

We detected a relatively high coverage of metabolites within the glutathione metabolism pathway. However, subtle variations of metabolites central to network topology, such as glutathione itself, were not differentially expressed resulting in the entire pathway being only marginally affected ( $p = 0.057$ ). On the other hand, the transulphuration pathway (cysteine and methionine metabolism) which is responsible for supplying precursor metabolites for glutathione synthesis under low-mid stress conditions was altered, which indicates a mild oxidative stress response. The subtle signs of oxidative stress and perturbed redox balance in virus-exposed larvae indicate that the homeostatic control mechanisms responsible for governing the production and detoxification of ROS were functioning at optimal capacities and well within acceptable boundaries. These findings suggest that OsHV-1 either does not induce major oxidative stress in oyster larvae beyond the adaptive ability of the ROS-regulatory system, or that the level or stage of infection in our study was low or early, respectively. These results also may highlight a potential limitation in the exclusive use of metabolomic-based approaches to recognise changes in metabolic activity under circumstances where enzymatic regulation tightly constrains metabolite levels within the range of normal baseline variations. Indeed, cellular metabolism, and glutathione turnover/ROS regulation in particular, is extremely well-adapted to achieve this feat. Thus, to better

define the influence of OsHV-1 on oxidative stress parameters, further analysis of enzymes associated with glutathione recycling and ROS regulation would be required.

#### 4.5 Other signatures

A number of other metabolites were considered to be important features responsible for larval health class discrimination in PCA, PLS-DA and RF models. These included elevated levels of 4-hydroxyphenylacetic acid, 4-hydroxyproline, and 2-aminoadipic acid and a reduction in nicotinic acid contents. Four unannotated metabolites were also important in the multivariate models. Future efforts to identify these molecules may further complement our interpretations or provide new insights into the virus-host interaction.

4-hydroxyphenylacetic acid (4-HPA) is a tyrosine-derived metabolite with antioxidant activity that can scavenge reactive oxygen and nitrogen species *in vitro* and *in vivo* (Biskup et al. 2013), and also has an ability to reduce excessive release of proinflammatory cytokines which protects against inflammation and disease (Liu et al. 2014; Ford et al. 2016). Increased levels of 4-HPA are associated with various mammalian disease pathologies and inborn errors in metabolism (Kikuchi et al. 2010; Nishiumi et al. 2010; Hori et al. 2011; Manna et al. 2015; Xiong et al. 2015; Kurko et al. 2016). An accumulation of this metabolite during such disease onsets has been attributed to differential catabolic pathways of tyrosine (Xiong et al. 2015). In our study, tyrosine metabolism was identified as a pathway with signs of being differentially regulated. It was recently demonstrated that the mechanism by which 4-HPA reduces proinflammatory cytokine production involves suppression of their transcription via promotion of HIF-1 $\alpha$  protein degradation (Liu et al. 2014). Thus, with a functional role in downregulating HIF-1 activity, 4-HPA could directly compete with *IrgI*/ITA/succinic acid-induced HIF-1 $\alpha$  stabilisation. As a result, HIF-1 induced enrichment of pathways responsible for redirecting carbon and nitrogen metabolism in trajectories which support OsHV-1

proliferation might be moderated, whereas the negative host consequences associated with co-induced respiratory dysfunction and excessive inflammation may partially be alleviated.

4-hydroxyproline (4-HP) is produced via the posttranslational hydroxylation of proline and is formed in proteins only after peptide linkage (Cooper et al. 2008). 4-HP is predominantly found in collagen, a major structural component of the extracellular matrix (ECM) scaffold in marine invertebrate embryos and larvae (Spiegel et al. 1989; Phang et al. 2010). Thus, accumulation of free 4-HP is a specific biomarker of collagen degradation, and indicator of cell structure damage through compositional transformation of the ECM (Karna & Palka 2002; Phang et al. 2008). The production of free 4-HP resulting from ECM degradation is thought to play a role in initiating the apoptotic cascade via activation of the caspase-9 protease (Cooper et al. 2008), as well as promoting HIF-1 activity by inhibiting the degradation of HIF-1 $\alpha$  (Surazynski et al. 2008). Matrix metalloproteinases (MMPs), are responsible for degrading the ECM. MMPs play crucial roles during normal embryonic and larval development, such as in cell growth and differentiation, tissue remodelling, and mechanisms of immunological defense (Mannello et al. 2003, 2005; Mok et al. 2009). However, MMPs can be excessively produced in pathological situations (Itoh et al. 2006; Phang et al. 2008). Physical stress, oncogenic transformation, ROS and cytokines are all inducible factors (Mancini & Battista 2006; Reuter et al. 2010). MMPs and their importance in restructuring the ECM as a response to pathogens have previously been implicated in OsHV-1 infections and disease resistance vs susceptibility traits of oysters (McDowell et al. 2014; Nikapitiya et al. 2014; Rosani et al. 2015). The elevated levels of free 4-HP in OsHV-1  $\mu$ Var-exposed larvae indicates that collagen degradation in the ECM was enhanced, although further investigation will be required to determine whether the 4-HP accumulations represent negative consequences for the host due to significant cell structure damage.

2-aminoadipic acid (2-AAA) is a component of the lysine metabolism pathway and is recognised as a small-molecule biomarker of oxidative stress (Sell et al. 2007; Zeitoun-Ghandour et al. 2011). Its presence has been linked with regulation of glucose homeostasis (Yuan et al. 2011; Wang et al. 2013), and elevated levels have been reported as a putative biosignature of respiration chain disorders (Smuts et al. 2013). Production of 2-AAA in fish is associated with low oxygen transport capacity (Allen et al. 2015), and can be induced in shellfish by exposure to physiological stressors (Chen et al. 2015; Koyama et al. 2015). Accumulations of 2-AAA are also associated with oncogene activation and carcinogenesis, leading to its recent candidacy as a potential new clinical biomarker for various cancers (Hori et al. 2011; Bellance et al. 2012; Jung et al. 2013; Rosi et al. 2015; Ren et al. 2016). Production of 2-AAA correlates with the bioenergetic signature characteristic of a switch in cellular respiration modes from OxPhos to aerobic glucose fermentation (Hori et al. 2011; Aa et al. 2012; Bellance et al. 2012). Thus, the accumulation of 2-AAA in virus-exposed larvae is consistent with the global changes we detected in organic acid metabolism reflective of TCA cycle reprogramming, reduced mitochondrial respiration and ATP production, activation of the Warburg effect, and subtle signs of oxidative stress.

Nicotinic acid (NA) plays an important role in redox reactions and can be converted to nicotinamide (NAM) *in vivo*. In invertebrates and some fish, NA and NAM are important precursors for synthesis of the pyrimidine nucleotide coenzymes  $\text{NAD}^+$  and  $\text{NADP}^+$  which participate in many hydrogen transfer processes, such as fatty acid synthesis, lipolysis and glycolysis (Ng et al. 1997; Sauve 2008; Houtkooper et al. 2009; Cantó et al. 2015; Yuasa & Ball 2015; Yuasa et al. 2015).  $\text{NAD}^+$  is also a substrate and signalling metabolite required for regulation of transcription, proteasomal function, and posttranslational protein modifications involved in DNA replication, recombination, repair mechanisms and maintenance of genomic stability (Bürkle 2001; Surjana et al. 2010; Vyas et al. 2013; Fouquerel & Sobol 2014; Cantó

et al. 2015). Unlike most metabolic redox reactions which reversibly oxidise or reduce pyrimidine nucleotides to maintain constant levels of  $\text{NAD}^+/\text{NADP}^+$ , substrate utilisation and  $\text{NAD}^+$ -dependant signalling processes are highly consumptive, and regeneration from niacin precursors is required when such mechanisms are activated (Lin 2007; Chiarugi et al. 2012). The reduction of free NA in virus-exposed larvae is consistent with its role in these processes which are upregulated during herpes-type viral infections (Grady et al. 2012; Li et al. 2012). Herpes-induced consumption of  $\text{NAD}^+$  as a substrate for enzymes involved in host DNA modifications is likely a response to DNA damage pathways being activated by replication of the viral genome (Grady et al. 2012). However, efficient virus replication itself and synthesis of viral proteins are also reliant on  $\text{NAD}^+$  substrate supply (Li et al. 2012). Thus, the importance of NA and  $\text{NAD}^+/\text{NADP}^+$  metabolism in host-pathogen interactions is gaining considerable attention as targets for the treatment of infectious diseases in humans (Mesquita et al. 2016). Interestingly, activation of the Warburg effect involves the unusual overproduction of  $\text{NAD}^+$  via enhanced fermentation of glucose (i.e., pyruvic acid +  $\text{NADH} \rightarrow \text{lactic acid} + \text{NAD}^+$ ) (Chiarugi et al. 2012), and may serve/function as a replenishing mechanism in response to  $\text{NAD}^+$  depletion to complement *de novo* synthesis from its niacin precursors.

#### 4.6 Study limitations

During an infection, viruses have an ability to alter host metabolites in order to benefit their replication. However, the host can also mount responses against the pathogen via changes in host metabolism pathways, such as triggering inflammation. Unfortunately, at this early stage of the research we do not know which metabolic features have roles in virus pathogenesis and which of the signatures can be attributed to host defence. This is an important aspect to decipher, and will require highly focused investigation. A critical step to achieve this will be



to characterise the functional genome of OsHV-1  $\mu$ Var. Furthermore, our study did not include a temporal sampling design. During an infection, viruses can trigger various metabolic changes at different replication stages. For example, the Warburg effect may be triggered at the stage of virus genome replication, whereas lipid metabolism may be altered at the stage of virion assembly prior to release of mature virion particles from host cells. In order to contextualise host metabolic perturbations within the framework of viral propagation, future efforts should be made to incorporate a fine scale temporal sampling design, analysis of multiple targets (genes, proteins and metabolites), and a detailed characterisation of the virus replication process; although, lack of bivalve cell lines continue to hamper virus research in these taxa (Yoshino & Bayne 2013).

## 5. CONCLUSION

In summary, we identified and measured the metabolic responses of oyster larvae during exposure to the virulent ostreid herpesvirus microvariant which has recently been responsible for mass mortalities of shellfish around the globe. Viruses can reshape their host's metabolism to create a unique metabolic state that supports their specific requirements. Indeed, profiling of larval metabolites revealed virus-induced reprogramming of host-encoded metabolic networks, including alterations to the glycolytic pathway, the TCA cycle, and lipid metabolism. Intriguingly, we observed metabolic response parallels with a number of innate immune system mechanisms previously characterised in mammalian cell models, such as induction of the Warburg effect and downstream metabolic consequences of immunoresponsive gene 1 like activation. The functional genomes of OsHV-1 and its variants are mostly unknown at present, but it is likely that virus-encoded auxiliary genes also provide infected host cells with novel metabolic capabilities, and the outcomes of their transcription may be manifested within our results. These findings provide the first



comprehensive insights into early ontogenic host physiology and susceptibility of oysters towards OsHV-1  $\mu$ Var. Characterisation of host-virus interactions can provide knowledge to enable development of therapeutic agents and identify traits for improving the outcome of selective breeding programmes. Our study also highlights the value of metabolomics-based approaches in elucidating host-virus interactions and the metabolic networks which characterise and underpin the pathophysiological state, and further supports its application for investigating pathogenesis of disease in early life stage oyster models.

#### ACKNOWLEDGEMENTS

We would like to thank the crew at the Cawthron Aquaculture Park for their support and guidance: Norman Ragg, Serean Adams, Zoë Hilton, Steve Webb, Samantha Gale, Henry Kaspar, and Mark Camara. We are thankful to the Aquaculture Biotechnology Group (AUT) for their input and support through this research. We are also thankful to Francesca Casu and Erica Zarate from University of Auckland for their technical assistance with sample analysis. We acknowledge support from an Auckland University of Technology Vice Chancellor Doctoral Scholarship to T. Young under the supervision of A.C. Alfaro. This work was funded by the New Zealand Ministry of Business, Innovation and Employment (CAWX0802 and CAWX1315).

## REFERENCES

- Aa, J., Yu, L., Sun, M., Liu, L., Li, M., Cao, B., et al., 2012. Metabolic features of the tumor microenvironment of gastric cancer and the link to the systemic macroenvironment. *Metabolomics*, 8(1), 164–173.
- Alfaro, A.C., Young, T., 2016. Showcasing metabolomics research in aquaculture: A review. *Rev. Aquacult.*, DOI: 10.1111/raq.12152
- Allen, P.J., Wise, D., Greenway, T., Khoo, L., Griffin, M.J., Jablonsky, M., 2015. Using 1-D  $^1\text{H}$  and 2-D  $^1\text{H}$  J-resolved NMR metabolomics to understand the effects of anemia in channel catfish (*Ictalurus punctatus*). *Metabolomics*, 11(5), 1131–1143.
- Apel, K., Hirt, H., 2004. Reactive oxygen species: Metabolism, oxidative stress, and signal transduction. *Annu. Rev. Plant Biol.*, 55, 373–399.
- Arzul, I., Nicolas, J.-L., Davison, A.J., Renault, T., 2001. French scallops: A new host for ostreid herpesvirus-1. *Virology*, 290, 342–349.
- Azéma P., Travers, M.A., Benabdelmouna, A., Dégremont, L., 2016. Single or dual experimental infections with *Vibrio aestuarianus* and OsHV-1 in diploid and triploid *Crassostrea gigas* at the spat, juvenile and adult stages. *J. Invertebr. Pathol.*, 139, 92–101.
- Bai, C., Gao, W., Wang, C., Yu, T., Zhang, T., Qiu, Z., et al., 2016. Identification and characterization of ostreid herpesvirus 1 associated with massive mortalities of *Scapharca broughtonii* broodstocks in China. *Dis. Aquat. Organ.*, 118(1), 65–75.
- Bai, C., Wang, C., Xia, J., Sun, H., Zhang, S., Huang, J., 2015. Emerging and endemic types of Ostreid herpesvirus 1 were detected in bivalves in China. *J. Invertebr. Pathol.*, 124, 98–106.
- Barnard, R., 2014. Determining the Need for a Multi-Species Mollusc Hatchery in Western Australia: ACWA Study Report. Australian Community Workers Association Mollusc Hatchery Report prepared by RMB Aqua, Albany, WA, Australia.
- Batista, F.M., López-Sanmartín, M., Grade, A., Morgado, I., Valente, M., Navas, J.I., et al., 2015. Sequence variation in ostreid herpesvirus 1 microvar isolates detected in dying and asymptomatic *Crassostrea angulata* adults in the Iberian Peninsula: Insights into viral origin and spread. *Aquaculture*, 435, 43–51.
- Bellance, N., Pabst, L., Allen, G., Rossignol, R., Nagraath, D., 2012. Oncosecretomics coupled to bioenergetics identifies  $\alpha$ -amino adipic acid, isoleucine and GABA as potential biomarkers of cancer: Differential expression of c-Myc, Oct1 and KLF4 coordinates metabolic changes. *BBA-Bioenergetics*, 1817(11), 2060–2071.
- Ben-Shlomo, I., Kol, S., Roeder, L.M., Resnick, C.E., Hurwitz, A., Payne, D.W., et al., 1997. Interleukin (IL)-1 $\beta$  increases glucose uptake and induces glycolysis in aerobically cultured rat ovarian cells: Evidence that IL-1 $\beta$  may mediate the gonadotropin-induced midcycle metabolic shift. *Endocrinology*, 138(7), 2680–2688.
- Bhatt, A.P., Jacobs, S.R., Freemerman, A.J., Makowski, L., Rathmell, J.C., Dittmer, D.P., et al., 2012. Dysregulation of fatty acid synthesis and glycolysis in non-Hodgkin lymphoma. *P. Natl. Acad. Sci. U. S. A.*, 109(29), 11818–11823.

- 793 Biskup, I., Golonka, I., Gamian, A., Sroka, Z., 2013. Antioxidant activity of selected phenols  
794 estimated by ABTS and FRAP methods. *Postep. Hig. Med. Dosw.*, 67, 958–963.
- 795 Bouhifd, M., Hartung, T., Hogberg, H.T., Kleensang, A., Zhao, L., 2013. Review:  
796 Toxicometabolomics. *J. Appl. Toxicol.*, 33(12), 1365–1383.
- 797 Braundmeier-Fleming, A., Russell, N.T., Yang, W., Nas, M.Y., Yaggie, R.E., Berry, M., et  
798 al., 2016. Stool-based biomarkers of interstitial cystitis/bladder pain syndrome. *Sci. Rep.*,  
799 DOI: 10.1038/srep26083
- 800 Burge, C.A., Griffin, F.J., Friedman, C.S., 2006. Mortality and herpesvirus infections of the  
801 Pacific oyster *Crassostrea gigas* in Tomales Bay, California, USA. *Dis. Aquat. Organ.*,  
802 72(1), 31–43.
- 803 Burge, C., Judah, L.R., Conquest, L.L., Griffin, F.J., Cheney, D.P., Suhrbier, A., et al., 2007.  
804 Summer seed mortality of the Pacific oyster, *Crassostrea gigas* Thunberg grown in  
805 Tomales Bay, California, U. S. A.: The influence of oyster stock, planting time,  
806 pathogens, and environmental stressors. *J. Shellfish Res.*, 26, 163–172.
- 807 Burge, C.A., Strenge, R.E., Friedman, C.S., 2011. Detection of the oyster herpesvirus in  
808 commercial bivalves in northern California, USA: Conventional and quantitative PCR.  
809 *Dis. Aquat. Organ.*, 94(2), 107–116.
- 810 Burge, C.A., Friedman, C.S., 2012. Quantifying ostreid herpesvirus (OsHV-1) genome copies  
811 and expression during transmission. *Microb. Ecol.*, 63(3), 596–604.
- 812 Burioli, E.A.V., Prearo, M., Riina, M.V., Bona, M.C., Fioravanti, M.L., Arcangeli, G., et al.,  
813 2016. Ostreid herpesvirus type 1 genomic diversity in wild populations of Pacific oyster  
814 *Crassostrea gigas* from Italian coasts. *J. Invertebr. Pathol.*, 137, 71–83.
- 815 Bürkle, A., 2001. Physiology and pathophysiology of poly (ADP-ribosyl) ation. *Bioessays*,  
816 23(9), 795–806.
- 817 Cameron, S.J., Lewis, K.E., Beckmann, M., Allison, G.G., Ghosal, R., Lewis, P.D., et al.,  
818 2016. The metabolomic detection of lung cancer biomarkers in sputum. *Lung Cancer*, 94,  
819 88–95.
- 820 Cantó, C., Menzies, K.J., Auwerx, J., 2015. NAD<sup>+</sup> metabolism and the control of energy  
821 homeostasis: A balancing act between mitochondria and the nucleus. *Cell Metab.*, 22(1),  
822 31–53.
- 823 Cascante, M., Marin, S., 2008. Metabolomics and fluxomics approaches. *Essays Biochem.*,  
824 45, 67–82.
- 825 Castinel, A., Fletcher, L., Dhand, N., Rubio, A., Whittington, R., Taylor, M., 2015. OsHV-1  
826 mortalities in Pacific Oysters in Australia and New Zealand: The Farmer's Story.  
827 Prepared for the Ministry of Business, Innovation and Employment (MBIE). Cawthron  
828 Report No. 2567. 48 p.
- 829 Chambers, J.W., Maguire, T.G., Alwine, J.C., 2010. Glutamine metabolism is essential for  
830 human cytomegalovirus infection. *J. Virol.*, 84(4), 1867–1873.
- 831 Chen, D.Q., Chen, H., Chen, L., Tang, D.D., Miao, H., Zhao, Y.Y., 2016a. Metabolomic  
832 application in toxicity evaluation and toxicological biomarker identification of natural  
833 product. *Chem.-Biol. Interact.*, 252, 114–130.
- 834 Chen, I.T., Lee, D.Y., Huang, Y.T., Kou, G.H., Wang, H.C., Chang, G.D., et al., 2016b. Six  
835 hours after infection, the metabolic changes induced by WSSV neutralize the host's  
836 oxidative stress defenses. *Sci. Rep.*, 6, Article number 27732.

- 837 Chen, S., Zhang, C., Xiong, Y., Tian, X., Liu, C., Jeevithan, E. et al., 2015. A GC-MS-based  
838 metabolomics investigation on scallop (*Chlamys farreri*) during semi-anhydrous living-  
839 preservation. *Innov. Food Sci. Emerg.*, 31, 185–195.
- 840 Chiang, E., Dang, O., Anderson, K., Matsuzawa, A., Ichijo, H., David, M., 2006. Cutting  
841 edge: Apoptosis-regulating signal kinase 1 is required for reactive oxygen species-  
842 mediated activation of IFN regulatory factor 3 by lipopolysaccharide. *J. Immunol.*,  
843 176(10), 5720–5724.
- 844 Chiarugi, A., Dölle, C., Felici, R., Ziegler, M., 2012. The NAD metabolome – a key  
845 determinant of cancer cell biology. *Nat. Rev. Cancer*, 12(11), 741–752.
- 846 Chukkapalli, V., Heaton, N.S., Randall, G., 2012. Lipids at the interface of virus–host  
847 interactions. *Curr. Opin. Microbiol.*, 15(4), 512–518.
- 848 Cooper, S.K., Pandhare, J., Donald, S.P., Phang, J.M., 2008. A novel function for  
849 hydroxyproline oxidase in apoptosis through generation of reactive oxygen species. *J.*  
850 *Biol. Chem.*, 283(16), 10485–10492.
- 851 Cordes, T., Wallace, M., Michelucci, A., Divakaruni, A.S., Sapcaru, S.C., Sousa, C., et al.,  
852 2016. Immunoresponsive gene 1 and itaconate inhibit succinate dehydrogenase to  
853 modulate intracellular succinate levels. *J. Biol. Chem.*, 291(27), 14274–14284.
- 854 Corporeau, C., Tamayo, D., Pernet, F., Quéré, C., Madec, S., 2014. Proteomic signatures of  
855 the oyster metabolic response to herpesvirus OsHV-1  $\mu$ Var infection. *J. Proteomics*, 109,  
856 176–187.
- 857 Darekar, S., Georgiou, K., Yurchenko, M., Yenamandra, S.P., Chachami, G., Simos, G., et  
858 al., 2012. Epstein-Barr virus immortalization of human B-cells leads to stabilization of  
859 hypoxia-induced factor 1 alpha, congruent with the Warburg effect. *PLOS ONE*, 7(7),  
860 e42072.
- 861 Davis, J., 2016. A National Industry Response to Pacific Oyster Mortality Syndrome  
862 (POMS). An Agribusiness Tasmanian report commissioned by Oysters Australia Ltd,  
863 Tasmania, Australia.
- 864 Davison, A.J., Trus, B.L., Cheng, N., Steven, A.C., Watson, M.S., Cunningham, C., et al.,  
865 2005. A novel class of herpesvirus with bivalve hosts. *J. Gen. Virol.*, 86(1), 41–53.
- 866 Dégremont, L., 2013. Size and genotype affect resistance to mortality caused by OsHV-1 in  
867 *Crassostrea gigas*. *Aquaculture*, 416, 129–134.
- 868 Dégremont, L., Lamy, J.B., Pépin, J.F., Travers, M.A., Renault, T., 2015a. New insight for  
869 the genetic evaluation of resistance to Ostreid herpesvirus infection, a worldwide disease,  
870 in *Crassostrea gigas*. *PLOS ONE*, 10(6), e0127917.
- 871 Dégremont, L., Nourry, M., Maurouard, E., 2015b. Mass selection for survival and resistance  
872 to OsHV-1 infection in *Crassostrea gigas* spat in field conditions: Response to selection  
873 after four generations. *Aquaculture*, 446, 111–121.
- 874 Dégremont, L., Morga, B., Trancart, S., Pépin, J.F., 2016. Resistance to OsHV-1 infection in  
875 *Crassostrea gigas* larvae. *Front. Mar. Sci.*, 3, DOI: 10.3389/fmars.2016.00015
- 876 Delgado, T., Sanchez, E.L., Camarda, R., Lagunoff, M., 2012. Global metabolic profiling of  
877 infection by an oncogenic virus: KSHV induces and requires lipogenesis for survival of  
878 latent infection. *PLOS Pathog.*, 8(8), e1002866.
- 879 DoA, 2015. AQUAVETPLAN disease strategy: Infection with ostreid herpesvirus-1  
880 microvariant (Version 1), In: Australian Aquatic Veterinary Emergency Plan

- 881 (AQUAVETPLAN). Australian Government Department of Agriculture (DoA),  
882 Canberra, ACT, Australia.
- 883 Domeneghetti, S., Varotto, L., Civettini, M., Rosani, U., Stauder, M., Pretto, T., et al., 2014.  
884 Mortality occurrence and pathogen detection in *Crassostrea gigas* and *Mytilus*  
885 *galloprovincialis* close-growing in shallow waters (Goro lagoon, Italy). Fish Shellfish  
886 Immunol., 41(1), 37–44.
- 887 Ellis, R.P., Spicer, J.I., Byrne, J.J., Sommer, U., Viant, M.R., White, D.A., et al., 2014. <sup>1</sup>H  
888 NMR metabolomics reveals contrasting response by male and female mussels exposed to  
889 reduced seawater pH, increased temperature, and a pathogen. Environ. Sci. Technol.,  
890 48(12), 7044–7052.
- 891 Evans, O., Hick, P., Whittington, R.J., 2016. Distribution of Ostreid herpesvirus-1 (OsHV-1)  
892 microvariant in seawater in a recirculating aquaculture system. Aquaculture, 458, 21–28.
- 893 Fan, W., Ye, Y., Chen, Z., Shao, Y., Xie, X., Zhang, W., et al., 2016. Metabolic product  
894 response profiles of *Cherax quadricarinatus* towards white spot syndrome virus  
895 infection. Dev. Comp. Immunol., 61, 236–241.
- 896 FAO, 2016b. Global Aquaculture Production dataset (online query).  
897 <http://www.fao.org/fishery/statistics/global-aquaculture-production/query/en> (accessed  
898 19.09.2016). Food and Agriculture Organisation of the United Nations (FAO), Fisheries  
899 and Aquaculture Department, Rome, Italy.
- 900 Ferreira, L.M., 2010. Cancer metabolism: The Warburg effect today. Exp. Mol. Pathol.,  
901 89(3), 372–380.
- 902 Feussner, I., Polle, A., 2015. What the transcriptome does not tell—proteomics and  
903 metabolomics are closer to the plants' patho-phenotype. Curr. Opin. Plant Biol., 26, 26–  
904 31.
- 905 Fiehn, O., 2002. Metabolomics – the link between genotypes and phenotypes. Plant Mol.  
906 Biol. Rep., 48(1–2), 155–171.
- 907 Fleury, E., Moal, J., Boulo, V., Daniel, J.Y., Mazurais, D., Hénaut, A., et al., 2010.  
908 Microarray-based identification of gonad transcripts differentially expressed between  
909 lines of Pacific oyster selected to be resistant or susceptible to summer mortality. Mar.  
910 Biotechnol., 12(3), 326–339.
- 911 Fleury, E., Huvet, A., 2012. Microarray analysis highlights immune response of Pacific  
912 oysters as a determinant of resistance to summer mortality. Mar. Biotechnol., 14(2), 203–  
913 217.
- 914 Ford, C.T., Richardson, S., McArdle, F., Lotito, S.B., Crozier, A., McArdle, A., et al., 2016.  
915 Identification of (poly) phenol treatments that modulate the release of pro-inflammatory  
916 cytokines by human lymphocytes. Br. J. Nutr., 115(10), 1699–1710.
- 917 Fouquerel, E., Sobol, R.W., 2014. ARTD1 (PARP1) activation and NAD<sup>+</sup> in DNA repair and  
918 cell death. DNA Repair, 23, 27–32.
- 919 Friedman, C.S., Estes, R.M., Stokes, N.A., Burge, C.A., Hargove, J.S., Barber, B.J., et al.,  
920 2005. Herpes virus in juvenile Pacific oysters *Crassostrea gigas* from Tomales Bay,  
921 California, coincides with summer mortality episodes. Dis. Aquat. Organ., 63, 33–41.
- 922 Garcia, C., Thébault, A., Dégremont, L., Arzul, I., Miossec, L., Robert, M., et al., 2011.  
923 OsHV-1 detection and relationship with *C. gigas* spat mortality in France between 1998  
924 and 2006. Vet. Res., 42, 73–84.



- 925 Gómez-Chiarri, M., Guo, X., Tanguy, A., He, Y., Proestou, D., 2015. The use of-omic tools  
926 in the study of disease processes in marine bivalve mollusks. *J. Invertebr. Pathol.*, 131,  
927 137–154.
- 928 Goodwin, C.M., Xu, S., Munger, J., 2015. Stealing the keys to the kitchen: Viral  
929 manipulation of the host cell metabolic network. *Trends Microbiol.*, 23(12), 789–798.
- 930 Grady, S.L., Hwang, J., Vastag, L., Rabinowitz, J.D., Shenk, T., 2012. Herpes simplex virus  
931 1 infection activates poly (ADP-ribose) polymerase and triggers the degradation of poly  
932 (ADP-ribose) glycohydrolase. *J. Virol.*, 86(15), 8259–8268.
- 933 Green, T.J., Robinson, N., Chataway, T., Benkendorff, K., O'Connor, W., Speck, P., 2014a.  
934 Evidence that the major hemolymph protein of the Pacific oyster, *Crassostrea gigas*, has  
935 antiviral activity against herpesviruses. *Antiviral Res.*, 110, 168–174.
- 936 Green, T.J., Montagnani, C., Benkendorff, K., Robinson, N., Speck, P., 2014b. Ontogeny and  
937 water temperature influences the antiviral response of the Pacific oyster, *Crassostrea*  
938 *gigas*. *Fish Shellfish Immunol.*, 36(1), 151–157.
- 939 Green, T.J., Rolland, J.L., Vergnes, A., Raftos, D., Montagnani, C., 2015. OsHV-1  
940 countermeasures to the Pacific oyster's anti-viral response. *Fish Shellfish Immunol.*,  
941 47(1), 435–443.
- 942 Grijalva-Chon, J.M., Castro-Longoria, R., Ramos-Paredes, J., Enríquez-Espinoza, T.L.,  
943 Mendoza-Cano, F., 2013. Detection of a new OsHV-1 DNA strain in the healthy Pacific  
944 oyster, *Crassostrea gigas* Thunberg, from the Gulf of California. *J. Fish Dis.*, 36(11),  
945 965–968.
- 946 He, Y., Jouaux, A., Ford, S.E., Lelong, C., Sourdain, P., Mathieu, M., et al., 2015.  
947 Transcriptome analysis reveals strong and complex antiviral response in a mollusc. *Fish*  
948 *Shellfish Immunol.*, 46(1), 131–144.
- 949 Hill, C.B., Taylor, J.D., Edwards, J., Mather, D., Langridge, P., Bacic, A., et al., 2015.  
950 Detection of QTL for metabolic and agronomic traits in wheat with adjustments for  
951 variation at genetic loci that affect plant phenology. *Plant Sci.*, 233, 143–154.
- 952 Holmes, E., Wilson, I.D., Nicholson, J.K., 2008. Metabolic phenotyping in health and  
953 disease. *Cell*, 134(5), 714–717.
- 954 Hong, J., Yang, L., Zhang, D., Shi, J., 2016. Plant metabolomics: An indispensable system  
955 biology tool for plant science. *Int. J. Mol. Sci.*, 17(6), E767, DOI: 10.3390/ijms17060767
- 956 Hori, S., Nishiumi, S., Kobayashi, K., Shinohara, M., Hatakeyama, Y., Kotani, Y., et al.,  
957 2011. A metabolomic approach to lung cancer. *Lung Cancer*, 74(2), 284–292.
- 958 Houtkooper, R.H., Cantó, C., Wanders, R.J., Auwerx, J., 2010. The secret life of NAD<sup>+</sup>: An  
959 old metabolite controlling new metabolic signaling pathways. *Endocr. Rev.*, 31(2), 194–  
960 223.
- 961 Hsieh, Y.C., Chen, Y.M., Li, C.Y., Chang, Y.H., Liang, S.Y., Lin, S.Y., et al., 2015. To  
962 complete its replication cycle, a shrimp virus changes the population of long chain fatty  
963 acids during infection via the PI3K-Akt-mTOR-HIF1 $\alpha$  pathway. *Dev. Comp. Immunol.*,  
964 53(1), 85–95.
- 965 Hwang, J.Y., Park, J.J., Yu, H.J., Hur, Y.B., Arzul, I., Couraleau, Y., et al., 2013. Ostreid  
966 herpesvirus 1 infection in farmed Pacific oyster larvae *Crassostrea gigas* (Thunberg) in  
967 Korea. *J. Fish Dis.*, 36(11), 969–972.

- 968 Itoh, M., Murata, T., Suzuki, T., Shindoh, M., Nakajima, K., Imai, K., et al., 2006.  
 969 Requirement of STAT3 activation for maximal collagenase-1 (MMP-1) induction by  
 970 epidermal growth factor and malignant characteristics in T24 bladder cancer cells.  
 971 *Oncogene*, 25(8), 1195–1204.
- 972 Jee, B.Y., Lee, S.J., Cho, M.Y., Lee, S.J., Kim, J.W., Choi, S.H., et al., 2013. Detection of  
 973 ostreid herpesvirus 1 from adult Pacific oysters *Crassostrea gigas* cultured in Korea. *J.*  
 974 *Kor. Fish. Aqua. Sci.*, 16(2), 131–135.
- 975 Jenkins, C., Hick, P., Gabor, M., Spiers, Z., Fell, S.A., Gu, X., et al., 2013. Identification and  
 976 characterisation of an ostreid herpesvirus-1 microvariant (OsHV-1  $\mu$ -var) in *Crassostrea*  
 977 *gigas* (Pacific oysters) in Australia. *Dis. Aquat. Organ.*, 105(2), 109–126.
- 978 Jha, A.K., Huang, S.C.C., Sergushichev, A., Lampropoulou, V., Ivanova, Y., Loginicheva,  
 979 E., et al., 2015. Network integration of parallel metabolic and transcriptional data  
 980 reveals metabolic modules that regulate macrophage polarization. *Immunity*, 42(3),  
 981 419–430.
- 982 Jung, K., Reszka, R., Kamlage, B., Bethan, B., Stephan, C., Lein, M., et al., 2013. Tissue  
 983 metabolite profiling identifies differentiating and prognostic biomarkers for prostate  
 984 carcinoma. *Int. J. Cancer*, 133(12), 2914–2924.
- 985 Kalantari, S., Nafar, M., Samavat, S., Parvin, M., Fatemeh, B., Barzi, F., 2016.  $^1\text{H}$  NMR-  
 986 based metabolomics exploring urinary biomarkers correlated with proteinuria in focal  
 987 segmental glomerulosclerosis: A pilot study. *Magn. Reson. Chem.*, 54(10), 821–826.
- 988 Kanehisa, M., Goto, S., 2000. KEGG: Kyoto Encyclopedia of Genes and Genomes. *Nucleic*  
 989 *Acids Res.*, 28, 27–30.
- 990 Karna, E., Pałka, J.A., 2002. Inhibitory effect of acetylsalicylic acid on metalloproteinase  
 991 activity in human lung adenocarcinoma at different stages of differentiation. *Eur. J.*  
 992 *Pharmacol.*, 443(1), 1–6.
- 993 Karnovsky, A., Weymouth, T., Hull, T., Tarcea, V.G., Scardoni, G., Laudanna, C., et al.,  
 994 2012. Metscape 2 bioinformatics tool for the analysis and visualization of metabolomics  
 995 and gene expression data. *Bioinformatics*, 28(3), 373–380.
- 996 Keeling, S.E., Brosnahan, C.L., Williams, R., Gias, E., Hannah, M., Bueno, R., et al., 2014.  
 997 New Zealand juvenile oyster mortality associated with ostreid herpesvirus 1—an  
 998 opportunistic longitudinal study. *Dis. Aquat. Organ.*, 109, 231–239.
- 999 Kelly, B., O'Neill, L.A., 2015. Metabolic reprogramming in macrophages and dendritic cells  
 1000 in innate immunity. *Cell Res.*, 25(7), 771–784.
- 1001 Kikuchi, K., Itoh, Y., Tateoka, R., Ezawa, A., Murakami, K., Niwa, T., 2010. Metabolomic  
 1002 analysis of uremic toxins by liquid chromatography/electrospray ionization-tandem mass  
 1003 spectrometry. *J. Chromatogr. B Biomed. Sci. Appl.*, 878(20), 1662–1668.
- 1004 Knight, J.A., 2000. Review: Free radicals, antioxidants, and the immune system. *Ann. Clin.*  
 1005 *Lab. Sci.*, 30(2), 145–158.
- 1006 Koyama, H., Okamoto, S., Watanabe, N., Hoshino, N., Jimbo, M., Yasumoto, K., et al., 2015.  
 1007 Dynamic changes in the accumulation of metabolites in brackish water clam *Corbicula*  
 1008 *japonica* associated with alternation of salinity. *Comp. Biochem. Physiol. B Biochem.*  
 1009 *Mol. Biol.*, 181, 59–70.

- 1010 Koyuncu, E., Purdy, J.G., Rabinowitz, J.D., Shenk, T., 2013. Saturated very long chain fatty  
1011 acids are required for the production of infectious human cytomegalovirus progeny.  
1012 PLOS Pathog., 9(5), e1003333.
- 1013 Kurko, J., Tringham, M., Tanner, L., Nantö-Salonen, K., Vähä-Mäkilä, M., Nygren, H., et al.,  
1014 2016. Imbalance of plasma amino acids, metabolites and lipids in patients with lysinuric  
1015 protein intolerance (LPI). Metabolism, 65(9), 1361–1375.
- 1016 Lampropoulou, V., Sergushichev, A., Bambouskova, M., Nair, S., Vincent, E.E.,  
1017 Loginicheva, E., et al., 2016. Itaconate links inhibition of succinate dehydrogenase with  
1018 macrophage metabolic remodeling and regulation of inflammation. Cell Metab., 24(1),  
1019 158–166.
- 1020 Lewis, T., Defenderfer, D., Zippel, B., 2012. Understanding and Planning for the Potential  
1021 Impacts of OsHV-1  $\mu$ Var on the Australian Pacific oyster Industry. Final report (FRDC  
1022 2011/043), 1 September 2012. RDS Partners, Hobart, Australia, pp. 1–21.
- 1023 Li, C.Y., Wang, Y.J., Huang, S.W., Cheng, C.S., Wang, H.C., 2016. Replication of the  
1024 shrimp virus WSSV depends on glutamate-driven anaplerosis. PLOS ONE, 11(1),  
1025 e0146902.
- 1026 Li, Z., Yamauchi, Y., Kamakura, M., Murayama, T., Goshima, F., Kimura, H., et al., 2012.  
1027 Herpes simplex virus requires poly (ADP-ribose) polymerase activity for efficient  
1028 replication and induces extracellular signal-related kinase-dependent phosphorylation  
1029 and ICP0-dependent nuclear localization of tankyrase 1. J. Virol., 86(1), 492–503.
- 1030 Lin, H., 2007. Nicotinamide adenine dinucleotide: beyond a redox coenzyme. Org. Biomol.  
1031 Chem., 5(16), 2541–2554.
- 1032 Lionel, D., Guyader, T., Tourbiez, D., Pépin, J.F., 2013. Is horizontal transmission of the  
1033 Ostreid herpesvirus OsHV-1 in *Crassostrea gigas* affected by unselected or selected  
1034 survival status in adults to juveniles? Aquaculture, 408, 51–57.
- 1035 Littlewood-Evans, A., Sarret, S., Apfel, V., Loesle, P., Dawson, J., Zhang, J., et al., 2016.  
1036 GPR91 senses extracellular succinate released from inflammatory macrophages and  
1037 exacerbates rheumatoid arthritis. J. Exp. Med., 213(9), 1655–1662.
- 1038 Liu, P.F., Liu, Q.H., Wu, Y., Jie, H., 2015. A pilot metabolic profiling study in  
1039 hepatopancreas of *Litopenaeus vannamei* with white spot syndrome virus based on  $^1\text{H}$   
1040 NMR spectroscopy. J. Invertebr. Pathol., 124, 51–56.
- 1041 Liu, Z., Xi, R., Zhang, Z., Li, W., Liu, Y., Jin, F., et al., 2014. 4-Hydroxyphenylacetic acid  
1042 attenuated inflammation and edema via suppressing HIF-1 $\alpha$  in seawater aspiration-  
1043 induced lung injury in rats. Int. J. Mol. Sci., 15(7), 12861–12884.
- 1044 Ma, Y.M., Yang, M.J., Wang, S., Li, H., Peng, X.X., 2015. Liver functional metabolomics  
1045 discloses an action of L-leucine against *Streptococcus iniae* infection in tilapias. Fish  
1046 Shellfish Immunol., 45(2), 414–421.
- 1047 Maldonado, E.N., Lemasters, J.J., 2012. Warburg revisited: Regulation of mitochondrial  
1048 metabolism by voltage-dependent anion channels in cancer cells. J. Pharmacol. Exp.  
1049 Ther., 342(3), 637–641.
- 1050 Mancini, A., di Battista, J.A., 2006. Transcriptional regulation of matrix metalloprotease gene  
1051 expression in health and disease. Front. Biosci., 11, 423–446.
- 1052 Manna, S.K., Thompson, M.D., Gonzalez, F.J., 2015. Application of mass spectrometry-  
1053 based metabolomics in identification of early noninvasive biomarkers of alcohol-induced



- 1054 liver disease using mouse model, In: Biological Basis of Alcohol-Induced Cancer.  
1055 Springer International Publishing AG, Switzerland, pp. 217–238.
- 1056 Mannello, F., Canesi, L., Faimali, M., Piazza, V., Gallo, G., Geraci, S., 2003.  
1057 Characterization of metalloproteinase-like activities in barnacle (*Balanus amphitrite*)  
1058 nauplii. *Comp. Biochem. Physiol. B Biochem. Mol. Biol.*, 135(1), 17–24.
- 1059 Mannello, F., Tonti, G., Papa, S., 2005. Are matrix metalloproteinases the missing link.  
1060 *Invertebrate Surviv. J.*, 2(69), 69–74.
- 1061 Martenot, C., Oden, E., Travaille, E., Malas, J.P., Houssin, M., 2010. Comparison of two  
1062 real-time PCR methods for detection of ostreid herpesvirus 1 in the Pacific oyster  
1063 *Crassostrea gigas*. *J. Virol. Methods*, 170(1), 86–89.
- 1064 Martenot, C., Lethuillier, O., Fourour, S., Oden, E., Trancart, S., Travaillé, E., et al., 2015.  
1065 Detection of undescribed ostreid herpesvirus 1 (OsHV-1) specimens from Pacific oyster,  
1066 *Crassostrea gigas*. *J. Invertebr. Pathol.*, 132, 182–189.
- 1067 Martenot, C., Segarra, A., Baillon, L., Faury, N., Houssin, M., Renault, T., 2016. In situ  
1068 localization and tissue distribution of ostreid herpesvirus 1 proteins in infected Pacific  
1069 oyster, *Crassostrea gigas*. *J. Invertebr. Pathol.*, 136, 124–135.
- 1070 Martín-Gómez, L., Villalba, A., Abollo, E., 2012. Identification and expression of immune  
1071 genes in the flat oyster *Ostrea edulis* in response to bonamiosis. *Gene*, 492(1), 81–93.
- 1072 Mazzon, M., Mercer, J., 2014. Lipid interactions during virus entry and infection. *Cell.*  
1073 *Microbiol.*, 16(10), 1493–1502.
- 1074 McDowell, I.C., Nikapitiya, C., Aguiar, D., Lane, C.E., Istrail, S., Gomez-Chiarri, M., 2014.  
1075 Transcriptome of American oysters, *Crassostrea virginica*, in response to bacterial  
1076 challenge: Insights into potential mechanisms of disease resistance. *PLOS ONE*, 9(8),  
1077 e105097.
- 1078 Meiser, J., Krämer, L., Sapcariu, S.C., Battello, N., Ghelfi, J., D'Herouel, A.F., et al., 2016.  
1079 Pro-inflammatory macrophages sustain pyruvate oxidation through pyruvate  
1080 dehydrogenase for the synthesis of itaconate and to enable cytokine expression. *J. Biol.*  
1081 *Chem.*, 291(8), 3932–3946.
- 1082 Mesquita, I., Varela, P., Belinha, A., Gaifem, J., Laforge, M., Vergnes, B., et al., 2016.  
1083 Exploring NAD<sup>+</sup> metabolism in host–pathogen interactions. *Cell. Mol. Life Sci.*, 73(6),  
1084 1225–1236.
- 1085 Mesri, E.A., Feitelson, M.A., Munger, K., 2014. Human viral oncogenesis: A cancer  
1086 hallmarks analysis. *Cell Host Microbe*, 15(3), 266–282.
- 1087 Michelucci, A., Cordes, T., Ghelfi, J., Pailot, A., Reiling, N., Goldmann, O., et al., 2013.  
1088 Immune-responsive gene 1 protein links metabolism to immunity by catalyzing itaconic  
1089 acid production. *P. Natl. Acad. Sci. U. S. A.*, 110(19), 7820–7825.
- 1090 Mills, E., O'Neill, L.A., 2014. Succinate: A metabolic signal in inflammation. *Trends Cell*  
1091 *Biol.*, 24(5), 313–320.
- 1092 Mills, E.L., O'Neill, L.A., 2016. Reprogramming mitochondrial metabolism in macrophages  
1093 as an anti-inflammatory signal. *Eur. J. Immunol.*, 46(1), 13–21.
- 1094 Milne, B., 2016. Outbreak of 'POMS' in Tasmanian hatchery offers new insight into ostreid  
1095 herpesvirus. *Hatchery Int.*, May 2016.

- 1096 Mineur, F., Provan, J., Arnott, G., 2015. Phylogeographical analyses of shellfish viruses:  
1097 Inferring a geographical origin for ostreid herpesviruses OsHV-1 (Malacoherpesviridae).  
1098 Mar. Biol., 162(1), 181–192.
- 1099 Mok, F.S., Thiagarajan, V., Qian, P.Y., 2009. Proteomic analysis during larval development  
1100 and metamorphosis of the spionid polychaete *Pseudopolydora vexillosa*. Proteome Sci.,  
1101 7(1), 1–11.
- 1102 Mortensen, S., Strand, Å., Bodvin, T., Alfjorden, A., Skår, C.K., Jelmert, A., et al., 2016.  
1103 Summer mortalities and detection of ostreid herpesvirus microvariant in Pacific oyster  
1104 *Crassostrea gigas* in Sweden and Norway. Dis. Aquat. Organ., 117(3), 171–176.
- 1105 Munger, J., Bennett, B.D., Parikh, A., Feng, X.J., McArdle, J., Rabitz H.A., et al., 2008.  
1106 Systems-level metabolic flux profiling identifies fatty acid synthesis as a target for  
1107 antiviral therapy. Nat. Biotechnol., 26(10), 1179–1186.
- 1108 Naujoks, J., Tabeling, C., Dill, B.D., Hoffmann, C., Brown, A.S., Kunze, M., et al., 2016.  
1109 IFNs modify the proteome of legionella-containing vacuoles and restrict infection via  
1110 IRG1-derived itaconic acid. PLOS Pathog., 12(2), e1005408.
- 1111 Németh, B., Doczi, J., Csete, D., Kacso, G., Ravasz, D., Adams, D., et al., 2016. Abolition of  
1112 mitochondrial substrate-level phosphorylation by itaconic acid produced by LPS-  
1113 induced Irg1 expression in cells of murine macrophage lineage. FASEB J., 30(1), 286–  
1114 300.
- 1115 Ng, W.K., Serrini, G., Zhang, Z., Wilson, R.P., 1997. Niacin requirement and inability of  
1116 tryptophan to act as a precursor of NAD<sup>+</sup> in channel catfish, *Ictalurus punctatus*.  
1117 Aquaculture, 152(1), 273–285.
- 1118 Nikapitiya, C., McDowell, I.C., Villamil, L., Muñoz, P., Sohn, S., Gomez-Chiarri, M., 2014.  
1119 Identification of potential general markers of disease resistance in American oysters,  
1120 *Crassostrea virginica* through gene expression studies. Fish Shellfish Immunol., 41(1),  
1121 27–36.
- 1122 Nikiforova, V.J., Willmitzer, L., 2007. Network visualization and network analysis, in:  
1123 Baginsky, S., Fernie, A.R. (Eds.), Plant Systems Biology. Birkhäuser Verlag, Basel,  
1124 Switerland, pp. 245–275..
- 1125 Nishiumi, S., Shinohara, M., Ikeda, A., Yoshie, T., Hatan, N., Kakuyama, S., et al., 2010.  
1126 Serum metabolomics as a novel diagnostic approach for pancreatic cancer.  
1127 Metabolomics, 6(4), 518–528.
- 1128 Normand, J., Li, R., Quillien, V., Nicolas, J.L., Boudry, P., Pernet, F., et al., 2014. Contrasted  
1129 survival under field or controlled conditions displays associations between mRNA levels  
1130 of candidate genes and response to OsHV-1 infection in the Pacific oyster *Crassostrea*  
1131 *gigas*. Mar. Genomics, 15, 95–102.
- 1132 O'Neill, L.A., 2015. A broken krebs cycle in macrophages. Immunity, 42(3), 393–394.
- 1133 O'Neill, L.A., Pearce, E.J., 2016. Immunometabolism governs dendritic cell and  
1134 macrophage function. J. Exp. Med., 213(1), 15–23.
- 1135 O'Neill, L.A., Kishton, R.J., Rathmell, J., 2016. A guide to immunometabolism for  
1136 immunologists. Nat. Rev. Immunol., 16, 553–565.
- 1137 Oden, E., Martenot, C., Berthaux, M., Travaillé, E., Malas, J.P., Houssin, M., 2011.  
1138 Quantification of ostreid herpesvirus 1 (OsHV-1) in *Crassostrea gigas* by real-time PCR:

- determination of a viral load threshold to prevent summer mortalities. *Aquaculture*, 317(1), 27–31.
- OIE, 2016. Infection with ostreid herpesvirus 1 microvariants, In: *Manual of Diagnostic Tests for Aquatic Animals*. World Organisation for Animal Health (OIE), Paris, France.
- Owens, L., Malham, S., 2015. Review of the RNA interference pathway in molluscs including some possibilities for use in bivalves in aquaculture. *J. Mar. Sci. Eng.*, 3(1), 87–99.
- Pallares-Méndez, R., Aguilar-Salinas, C.A., Cruz-Bautista, I., del Bosque-Plata, L., 2016. Metabolomics in diabetes, a review. *Ann. Med.*, 48(1–2), 89–102.
- Palsson-McDermott, E.M., O'Neill, L.A., 2013. The Warburg effect then and now: From cancer to inflammatory diseases. *Bioessays*, 35(11), 965–973.
- Paul-Pont, I., Dhand, N.K., Whittington, R.J., 2013. Influence of husbandry practices on OsHV-1 associated mortality of Pacific oysters *Crassostrea gigas*. *Aquaculture*, 412, 202–214.
- Paul-Pont, I., Evans, O., Dhand, N.K., Whittington, R.J., 2015. Experimental infections of Pacific oyster *Crassostrea gigas* using the Australian OsHV-1  $\mu$ Var strain. *Dis. Aquat. Organ.*, 113(2), 137–147.
- Pernet, F., Barret, J., Marty, C., Moal, J., Le Gall, P., Boudry, P., 2010. Environmental anomalies, energetic reserves and fatty acid modifications in oysters coincide with an exceptional mortality event. *Mar. Ecol. Prog. Ser.*, 401, 129–46.
- Pernet, F., Lagarde, F., Jeannée, N., Daigle, G., Barret, J., Le Gall, P., et al., 2014. Spatial and temporal dynamics of mass mortalities in oysters is influenced by energetic reserves and food quality. *PLOS ONE*, 9, e88469.
- Petton, B., Pernet, F., Robert, R., Boudry, P., 2013. Temperature influence on pathogen transmission and subsequent mortalities in juvenile Pacific oysters *Crassostrea gigas*. *Aquacult. Env. Interac.*, 3, 257–273.
- Phang, J.M., Donald, S.P., Pandhare, J., Liu, Y., 2008. The metabolism of proline, a stress substrate, modulates carcinogenic pathways. *Amino Acids*, 35(4), 681–690.
- Phang, J.M., Liu, W., Zabirnyk, O., 2010. Proline metabolism and microenvironmental stress. *Annu. Rev. Nutr.*, 30, 441–463.
- Pisoschi, A.M., Pop, A., 2015. The role of antioxidants in the chemistry of oxidative stress: A review. *Eur. J. Med. Chem.*, 97, 55–74.
- Preusse, M., Tantawy, M.A., Klawonn, F., Schughart, K., Pessler, F., 2013. Infection-and procedure-dependent effects on pulmonary gene expression in the early phase of influenza A virus infection in mice. *BMC Microbiol.*, 13(1), 293, DOI: 10.1186/1471-2180-13-293
- Purdy, J.G., Shenk, T., Rabinowitz, J.D., 2015. Fatty Acid elongase 7 catalyzes lipidome remodeling essential for human cytomegalovirus replication. *Cell Rep.*, 10(8), 1375–1385.
- Ragg, N.L., King, N., Watts, E., Morrish, J., 2010. Optimising the delivery of the key dietary diatom *Chaetoceros calcitrans* to intensively cultured Greenshell™ mussel larvae, *Perna canaliculus*. *Aquaculture*, 306(1), 270–280.

- 1181 Ren, S., Shao, Y., Zhao, X., Hong, C.S., Wang, F., Lu, X., et al., 2016. Integration of  
1182 metabolomics and transcriptomics reveals major metabolic pathways and potential  
1183 biomarker involved in prostate cancer. *Mol. Cell. Proteomics*, 15(1), 154–163.
- 1184 Ren, W., Chen, H., Renault, T., Cai, Y., Bai, C., Wang, C., et al., 2013. Complete genome  
1185 sequence of acute viral necrosis virus associated with massive mortality outbreaks in the  
1186 Chinese scallop, *Chlamys farreri*. *Viol. J.*, 10(1), 110, DOI: 10.1186/1743-422X-10-110
- 1187 Renault, T., Le Deuff, R.M., Cochenne, N., Chollet, B., Maffart, P., 1995. Herpes-like  
1188 viruses associated with high mortality levels in larvae and spat of Pacific oysters,  
1189 *Crassostrea gigas*: A comparative study, the thermal effects on virus detection in  
1190 hatchery-reared larvae, reproduction of the disease in axenic larvae. *Vet. Res.*, 26(5–6),  
1191 539–43.
- 1192 Renault, T., Arzul, I., 2001. Herpes-like virus infections in hatchery-reared bivalve larvae in  
1193 Europe: Specific viral DNA detection by PCR. *J. Fish Dis.*, 24(3), 161–168.
- 1194 Renault, T., Faury, N., Barbosa-Solomieu, V., Moreau, K., 2011. Suppression subtractive  
1195 hybridisation (SSH) and real time PCR reveal differential gene expression in the Pacific  
1196 cupped oyster, *Crassostrea gigas*, challenged with Ostreid herpesvirus 1. *Dev. Comp.*  
1197 *Immunol.*, 35(7), 725–735.
- 1198 Renault, T., Moreau, P., Faury, N., Pepin, J.F., Segarra, A., Webb, S., 2012. Analysis of  
1199 clinical Ostreid herpesvirus 1 (Malacoherpesviridae) specimens by sequencing amplified  
1200 fragments from three virus genome areas. *J. Virol.*, 86(10), 5942–5947.
- 1201 Renault, T., Tchaleu, G., Faury, N., Moreau, P., Segarra, A., Barbosa-Solomieu, V., et al.,  
1202 2014. Genotyping of a microsatellite locus to differentiate clinical Ostreid herpesvirus 1  
1203 specimens. *Vet. Res.*, 45(1), 1–8.
- 1204 Reuter, S., Gupta, S.C., Chaturvedi, M.M., Aggarwal, B.B., 2010. Oxidative stress,  
1205 inflammation, and cancer: How are they linked? *Free Radic. Biol. Med.*, 49(11), 1603–  
1206 1616.
- 1207 Rosani, U., Varotto, L., Domeneghetti, S., Arcangeli, G., Pallavicini, A., Venier, P., 2015.  
1208 Dual analysis of host and pathogen transcriptomes in ostreid herpesvirus 1-positive  
1209 *Crassostrea gigas*. *Environ. Microbiol.*, 17(11), 4200–4212.
- 1210 Rosenwasser, S., Ziv, C., van Creveld, S.G., Vardi, A., 2016. Virocell metabolism: Metabolic  
1211 innovations during host–virus interactions in the ocean. *Trends Microbiol.*, 24(10), 821–  
1212 832.
- 1213 Rosi, A., Ricci-Vitiani, L., Biffoni, M., Grande, S., Luciani, A.M., Palma, A., et al., 2015. <sup>1</sup>H  
1214 NMR spectroscopy of glioblastoma stem-like cells identifies alpha-amino adipate as a  
1215 marker of tumor aggressiveness. *NMR Biomed.*, 28(3), 317–326.
- 1216 Rubic, T., Lametschwandner, G., Jost, S., Hinteregger, S., Kund, J., Carballido-Perrig, N., et  
1217 al., 2008. Triggering the succinate receptor GPR91 on dendritic cells enhances  
1218 immunity. *Nat. Immunol.*, 9(11), 1261–1269.
- 1219 Sanchez, E.L., Carroll, P.A., Thalhoffer, A.B., Lagunoff, M., 2015. Latent KSHV infected  
1220 endothelial cells are glutamine addicted and require glutaminolysis for survival. *PLOS*  
1221 *Pathog.*, 11(7), e1005052.
- 1222 Sanchez, E.L., Lagunoff, M., 2015. Viral activation of cellular metabolism. *Virology*, 479,  
1223 609–618.

- 1224 Sanmartín, M.L., Power, D.M., de la Herrán, R., Navas, J.I., Batista, F.M., 2016.  
 1225 Experimental infection of European flat oyster *Ostrea edulis* with ostreid herpesvirus 1  
 1226 microvar (OsHV-1 $\mu$ var): Mortality, viral load and detection of viral transcripts by in situ  
 1227 hybridization. *Virus Res.*, 217, 55–62.
- 1228 Sauve, A.A., 2008. NAD<sup>+</sup> and vitamin B3: From metabolism to therapies. *J. Pharmacol. Exp.*  
 1229 *Ther.*, 324(3), 883–893.
- 1230 Schikorski, D., Faury, N., Pépin, J.F., Saulnier, D., Tourbiez, D., Renault, T., 2011a.  
 1231 Experimental ostreid herpesvirus 1 infection of the Pacific oyster *Crassostrea gigas*:  
 1232 Kinetics of virus DNA detection by q-PCR in seawater and in oyster samples. *Virus*  
 1233 *Res.*, 155, 28–34.
- 1234 Schikorski, D., Renault, T., Saulnier, D., Faury, N., Moreau, P., Pépin, J.F., 2011b.  
 1235 Experimental infection of Pacific oyster *Crassostrea gigas* spat by ostreid herpesvirus 1:  
 1236 Demonstration of oyster spat susceptibility. *Vet. Res.*, 42(1), 27, DOI: 10.1186/1297-  
 1237 9716-42-27
- 1238 Schmitt, P., Santini, A., Vergnes, A., Degremont, L., de Lorgeril, J., 2013. Sequence  
 1239 polymorphism and expression variability of *Crassostrea gigas* immune related genes  
 1240 discriminate two oyster lines contrasted in term of resistance to summer mortalities.  
 1241 *PLOS ONE*, 8(9), e75900.
- 1242 Segarra, A., Pépin, J.F., Arzul, I., Morga, B., Faury, N., Renault, T., 2010. Detection and  
 1243 description of a particular Ostreid herpesvirus 1 genotype associated with massive  
 1244 mortality outbreaks of Pacific oysters, *Crassostrea gigas*, in France in 2008. *Virus Res.*,  
 1245 153(1), 92–99.
- 1246 Segarra, A., Baillon, L., Tourbiez, D., Benabdelmouna, A., Faury, N., Bourgougnon, N., et  
 1247 al., 2014a. Ostreid herpesvirus type 1 replication and host response in adult Pacific  
 1248 oysters, *Crassostrea gigas*. *Vet. Res.*, 45(1), 103, DOI: 10.1186/s13567-014-0103-x
- 1249 Segarra, A., Mauduit, F., Faury, N., Trancart, S., Dégremont, L., Tourbiez, D., et al., 2014b.  
 1250 Dual transcriptomics of virus-host interactions: Comparing two Pacific oyster families  
 1251 presenting contrasted susceptibility to ostreid herpesvirus 1. *BMC Genomics*, 15(1), 580.
- 1252 Segarra, A., Baillon, L., Faury, N., Tourbiez, D., Renault, T., 2016. Detection and  
 1253 distribution of ostreid herpesvirus 1 in experimentally infected Pacific oyster spat. *J.*  
 1254 *Invertebr. Pathol.*, 133, 59–65.
- 1255 Selak, M.A., Armour, S.M., MacKenzie, E.D., Boulahbel, H., Watson, D.G., Mansfield,  
 1256 K.D., et al., 2005. Succinate links TCA cycle dysfunction to oncogenesis by inhibiting  
 1257 HIF- $\alpha$  prolyl hydroxylase. *Cancer Cell*, 7(1), 77–85.
- 1258 Sell, D.R., Strauch, C.M., Shen, W., Monnier, V.M., 2007. 2-Aminoadipic acid is a marker of  
 1259 protein carbonyl oxidation in the aging human skin: Effects of diabetes, renal failure and  
 1260 sepsis. *Biochem J.*, 404(2), 269–277.
- 1261 Semenza, G.L., 2010. HIF-1: Upstream and downstream of cancer metabolism. *Curr. Opin.*  
 1262 *Genet. Dev.*, 20(1), 51–56.
- 1263 Senyilmaz, D., Teleman, A.A., 2015. Chicken or the egg: Warburg effect and mitochondrial  
 1264 dysfunction. *F1000Prime Rep.*, 7: 41, DOI: 10.12703/P7-41
- 1265 Seo, J.Y., Cresswell, P., 2013. Viperin regulates cellular lipid metabolism during human  
 1266 cytomegalovirus infection. *PLOS Pathog.*, 9(8), e1003497.



- 1267 Sévin, D.C., Kuehne, A., Zamboni, N., Sauer, U., 2015. Biological insights through  
1268 nontargeted metabolomics. *Curr. Opin. Biotechnol.*, 34, 1–8.
- 1269 Shannon, P., Markiel, A., Ozier, O., Baliga, N.S., Wang, J.T., Ramage, D., et al., 2003.  
1270 Cytoscape: A software environment for integrated models of biomolecular interaction  
1271 networks. *Genome Res.*, 13(11), 2498–504.
- 1272 Shimahara, Y., Kurita, J., Kiryu, I., Nishioka, T., Yuasa, K., Kawana, M., et al., 2012.  
1273 Surveillance of type 1 ostreid herpesvirus (OsHV-1) variants in Japan. *Fish Pathol.*,  
1274 47(4), 129–136.
- 1275 Villas-Bôas, S.G., Smart, K.F., Sivakumaran, S., Lane, G.A., 2011. Alkylation or silylation  
1276 for analysis of amino and non-amino organic acids by GC-MS?. *Metabolites*, 1(1), 3–20.
- 1277 Smuts, I., Van der Westhuizen, F.H., Louw, R., Mienie, L.J., Engelke, U.F., Wevers, R.A., et  
1278 al., 2013. Disclosure of a putative biosignature for respiratory chain disorders through a  
1279 metabolomics approach. *Metabolomics*, 9(2), 379–391.
- 1280 Spencer, C.M., Schafer, X.L., Moorman, N.J., Munger, J., 2011. Human cytomegalovirus  
1281 induces the activity and expression of acetyl-coenzyme A carboxylase, a fatty acid  
1282 biosynthetic enzyme whose inhibition attenuates viral replication. *J. Virol.*, 85(12),  
1283 5814–5824.
- 1284 Spiegel, E., Howard, L., Spiegel, M., 1989. Extracellular matrix of sea urchin and other  
1285 marine invertebrate embryos. *J. Morphol.*, 199(1), 71–92.
- 1286 Stehbens, W.E., 2004. Oxidative stress in viral hepatitis and AIDS. *Exp. Mol. Pathol.*, 77(2),  
1287 121–132.
- 1288 Størseth, T.R., Hammer, K.M., 2014. Environmental metabolomics of aquatic organisms.  
1289 *eMagRes*, 2(4), DOI: 10.1002/9780470034590
- 1290 Su, M.A., Huang, Y.T., Chen, I.T., Lee, D.Y., Hsieh, Y.C., Li, C.Y., et al., 2014. An  
1291 invertebrate Warburg effect: A shrimp virus achieves successful replication by altering  
1292 the host metabolome via the PI3K-Akt-mTOR pathway. *PLOS Pathog.*, 10(6), e1004196.
- 1293 Surazynski, A., Donald, S.P., Cooper, S.K., Whiteside, M.A., Salnikow, K., Liu, Y., et al.,  
1294 2008. Extracellular matrix and HIF-1 signaling: The role of prolidase. *Int. J. Cancer*,  
1295 122(6), 1435–1440.
- 1296 Surjana, D., Halliday, G.M., Damian, D.L., 2010. Role of nicotinamide in DNA damage,  
1297 mutagenesis, and DNA repair. *J. Nucleic Acids*, Article ID 157591, DOI:  
1298 10.4061/2010/157591
- 1299 Tallam, A., Perumal, T.M., Antony, P.M., Jäger, C., Fritz, J.V., Vallar, L., et al., 2016. Gene  
1300 Regulatory Network Inference of Immunoresponsive Gene 1 (IRG1) Identifies Interferon  
1301 Regulatory Factor 1 (IRF1) as Its Transcriptional Regulator in Mammalian  
1302 Macrophages. *PLOS ONE*, 11(2), e0149050.
- 1303 Tamayo, D., Corporeau, C., Petton, B., Quéré, C., Pernet, F., 2014. Physiological changes in  
1304 Pacific oyster *Crassostrea gigas* exposed to the herpesvirus OsHV-1  $\mu$ var. *Aquaculture*,  
1305 432, 304–310.
- 1306 Tannahill, G.M., Curtis, A.M., Adamik, J., Palsson-McDermott, E.M., McGettrick, A.F.,  
1307 Goel, G., et al., 2013. Succinate is an inflammatory signal that induces IL-1 [bgr]  
1308 through HIF-1 [agr]. *Nature*, 496(7444), 238–242.

- 1309 Thai, M., Graham, N.A., Braas, D., Nehil, M., Komisopoulou, E., Kurdistani, S.K., et al.,  
1310 2014. Adenovirus E4ORF1-induced MYC activation promotes host cell anabolic glucose  
1311 metabolism and virus replication. *Cell Metab.*, 19(4), 694–701.
- 1312 Thai, M., Thaker, S.K., Feng, J., Du, Y., Hu, H., Wu, T.T., et al., 2015. MYC-induced  
1313 reprogramming of glutamine catabolism supports optimal virus replication. *Nat.*  
1314 *Commun.*, 6, Article number 8873, DOI: 10.1038/ncomms9873
- 1315 Thompson, C.B., 2014. Wnt meets Warburg: Another piece in the puzzle? *EMBO J.*, 33(13),  
1316 1420–1422.
- 1317 Tilford, C.A., Siemers, N.O., 2009. Gene set enrichment analysis, in: Nikolsky Y., Bryant J.  
1318 (Eds.), *Protein Networks and Pathway Analysis*. Humana Press, Springer, New York,  
1319 USA, pp. 99–121.
- 1320 Torres, M.A., Jones, J.D., Dangl, J.L., 2006. Reactive oxygen species signaling in response to  
1321 pathogens. *Plant Physiol.*, 141(2), 373–378.
- 1322 Touw, W.G., Bayjanov, J.R., Overmars, L., Backus, L., Boekhorst, J., Wels, M., et al., 2012.  
1323 Data mining in the life sciences with Random Forest: A walk in the park or lost in the  
1324 jungle? *Brief. Bioinform.*, 14 (3), 315–326.
- 1325 Tretter, L., Patocs, A., Chinopoulos, C., 2016. Succinate, an intermediate in metabolism,  
1326 signal transduction, ROS, hypoxia, and tumorigenesis. *BBA-Bioenergetics*, 1857(8),  
1327 1086–1101.
- 1328 Vander, Heiden, M.G., Cantley, L.C., Thompson, C.B., 2009. Understanding the Warburg  
1329 effect: The metabolic requirements of cell proliferation. *Science*, 324(5930), 1029–1033.
- 1330 Vijayakumar, S.N., Sethuraman, S., Krishnan, U.M., 2015. Metabolic pathways in cancers:  
1331 Key targets and implications in cancer therapy. *RSC Adv.*, 5(52), 41751–41762.
- 1332 Vuoristo, K.S., Mars, A.E., van Loon, S., Orsi, E., Eggink, G., Sanders, J.P., et al., 2015.  
1333 Heterologous expression of *Mus musculus* immunoresponsive gene 1 (*irg1*) in  
1334 *Escherichia coli* results in itaconate production. *Front. Microbiol.*, 6, 849, DOI:  
1335 10.3389/fmicb.2015.00849
- 1336 Vyas, S., Chesarone-Cataldo, M., Todorova, T., Huang, Y.H., Chang, P., 2013. A systematic  
1337 analysis of the PARP protein family identifies new functions critical for cell physiology.  
1338 *Nat. Commun.*, 4 Article number 2240, DOI: 10.1038/ncomms3240
- 1339 Wang, T.J., Ngo, D., Psychogios, N., Dejam, A., Larson, M.G., Vasan, R.S., et al., 2013. 2-  
1340 Amino adipic acid is a biomarker for diabetes risk. *J. Clin. Invest.*, 123(10), 4309–4317.
- 1341 Weljie, A.M., Jirik, F.R., 2011. Hypoxia-induced metabolic shifts in cancer cells: Moving  
1342 beyond the Warburg effect. *Int. J. Biochem. Cell Biol.*, 43(7), 981–989.
- 1343 Whittington, R., Hick, P., Evans, O., Rubio, A., Dhand, N., Paul-Pont, I., 2016. Pacific oyster  
1344 mortality syndrome: A marine herpesvirus active in Australia. *Microbiol. Aust.*, 37(3),  
1345 126–128.
- 1346 Winter, G., Krömer, J.O., 2013. Fluxomics—connecting ‘omics analysis and phenotypes.  
1347 *Environ. Microbiol.*, 15(7), 1901–1916.
- 1348 Wishart, D.S., 2016. Emerging applications of metabolomics in drug discovery and precision  
1349 medicine. *Nat. Rev. Drug Discov.*, 15, 473–484.

- 1350 Wu, H., Ji, C., Wei, L., Zhao, J., Lu, H., 2013. Proteomic and metabolomic responses in  
1351 hepatopancreas of *Mytilus galloprovincialis* challenged by *Micrococcus luteus* and  
1352 *Vibrio anguillarum*. J. Proteomics, 94, 54–67.
- 1353 Xia, J., Wishart, D.S., 2010. MetPA: A web-based metabolomics tool for pathway analysis  
1354 and visualization. Bioinformatics, 26(18), 2342–2344.
- 1355 Xia, J., Wishart, D.S., 2011. Web-based inference of biological patterns, functions and  
1356 pathways from metabolomic data using MetaboAnalyst. Nat. Protoc., 6, 743–760.
- 1357 Xia, J., Bai, C., Wang, C., Song, X., Huang, J., 2015a. Complete genome sequence of Ostreid  
1358 herpesvirus-1 associated with mortalities of *Scapharca broughtonii* broodstocks. Virol.  
1359 J., 12(1), 110–119.
- 1360 Xia, J., Sinelnikov, I.V., Han, B., Wishart, D.S., 2015b. MetaboAnalyst 3.0—making  
1361 metabolomics more meaningful. Nucleic Acid Res., 43(W1), W251–W257.
- 1362 Xiong, X., Sheng, X., Liu, D., Zeng, T., Peng, Y., Wang, Y., 2015. A GC/MS-based  
1363 metabolomic approach for reliable diagnosis of phenylketonuria. Anal. Bioanal. Chem.,  
1364 407(29), 8825–8833.
- 1365 Yamamoto, K., Nagata, K., Ohara, H., Aso, Y., 2015. Challenges in the production of  
1366 itaconic acid by metabolically engineered *Escherichia coli*. Bioengineered, 6(5), 303–  
1367 306.
- 1368 Ye, Y., Xia, M., Mu, C., Li, R., Wang, C., 2016. Acute metabolic response of *Portunus*  
1369 *trituberculatus* to *Vibrio alginolyticus* infection. Aquaculture, 463, 201–208.
- 1370 Yoshino, T.P., Bickham, U., Bayne, C.J., 2013. Molluscan cells in culture: Primary cell  
1371 cultures and cell lines 1. Can. J. Zool., 91(6), 391–404.
- 1372 Young, T., Alfaro, A.C., Villas-Boas, S.G., 2015. Identification of candidate biomarkers for  
1373 quality assessment of hatchery-reared mussel larvae via GC/MS-based metabolomics. N.  
1374 Z. J. Mar. Freshwater Res., 49(1), 87–95.
- 1375 Young, T., Alfaro, A.C., 2016. Metabolomic strategies for aquaculture research: A primer.  
1376 Rev. Aquacult., DOI: 10.1111/raq.12146
- 1377 Young, T., Alfaro, A.C., Villas-Boas, S.G., 2016. Metabolic profiling of mussel larvae:  
1378 Effect of handling and culture conditions. Aquacult. Int., 24(3), pp. 843–856.
- 1379 Yuan, W., Zhang, J., Li, S., Edwards, J.L., 2011. Amine metabolomics of hyperglycemic  
1380 endothelial cells using capillary LC–MS with isobaric tagging. J. Proteome Res., 10(11),  
1381 5242–5250.
- 1382 Yuasa, H.J., Ball, H.J., 2015. Efficient tryptophan-catabolizing activity is consistently  
1383 conserved through evolution of TDO enzymes, but not IDO enzymes. J. Exp. Zool. B  
1384 Mol. Dev. Evol., 324(2), 128–140.
- 1385 Yuasa, H.J., Mizuno, K., Ball, H.J., 2015. Low efficiency IDO2 enzymes are conserved in  
1386 lower vertebrates, whereas higher efficiency IDO1 enzymes are dispensable. FEBS J.,  
1387 282(14), 2735–2745.
- 1388 Zaidi, N., Lupien, L., Kuemmerle, N.B., Kinlaw, W.B., Swinnen, J.V., Smans, K., 2013.  
1389 Lipogenesis and lipolysis: The pathways exploited by the cancer cells to acquire fatty  
1390 acids. Prog. Lipid Res., 52(4), 585–589.



- 1391 Zeitoun-Ghandour, S., Leszczyszyn, O.I., Blindauer, C.A., Geier, F.M., Bundy, J.G.,  
1392 Stürzenbaum, S.R., 2011. *C. elegans* metallothioneins: Response to and defence against  
1393 ROS toxicity. *Mol. Biosyst.*, 7(8), 2397–2406.
- 1394 Zhang, J., Nuebel, E., Daley, G.Q., Koehler, C.M., Teitell, M.A., 2012. Metabolic regulation  
1395 in pluripotent stem cells during reprogramming and self-renewal. *Cell Stem Cell*, 11(5),  
1396 589–595.
- 1397 Zhao, X.L., Han, Y., Ren, S.T., Ma, Y.M., Li, H., Peng, X.X., 2015. L-proline increases  
1398 survival of tilapias infected by *Streptococcus agalactiae* in higher water temperature.  
1399 *Fish Shellfish Immunol.*, 44(1), 33–42.

**Figure 1.** Metabolites detected as being significantly different ( $p < 0.05$ ) between control and OsHV-1  $\mu$ Var-infected larvae. (A) Significant Analysis of Metabolites (SAM) plot. (B) Empirical Bayes Analysis of Metabolites (EBAM) plot. (C) Summary of statistically different metabolite levels between treatment groups with their respective  $\text{Log}_2$  fold change values (virus-infected [red circles] / control [green circles] larvae).

**Figure 2.** Unsupervised multivariate cluster analyses of metabolite profiles from larvae infected with OsHV-1  $\mu$ Var vs control larvae. (A) Hierarchical Cluster Analysis (Euclidian distance; Ward's method). (B) Table of results from  $k$ -Means cluster analysis where  $k$  clusters = 2 ( $Cn$  = control sample  $n$ ;  $Vn$  = virus-infected sample  $n$ ). (C) Principal Component Analysis (PCA) score plot. (D) PCA scree plot showing variation explained by  $n$  PC (blue line), and the cumulative variance explained in  $n$  PC's (green line).

**Figure 3.** Supervised multivariate classification analyses of metabolite profiles from larvae infected with OsHV-1  $\mu$ Var vs control larvae. (A) Projection to Latent Structure Discriminant Analysis (PLS-DA) score plot with accuracy of 100%, multiple correlation coefficient ( $R^2$ ) of 96.9%, and cross-validated  $R^2$  ( $Q^2$ ) of 79.6%. (B) Variable Importance in Projection (VIP) scores for the PLS-DA model.

**Figure 4.** Multivariate machine learning and predictive modelling of larval sample classes via Random Forest (RF) analysis with Monte-Carlo Cross Validation (MCCV). (A) Predictive accuracies of RF models with different  $n$  features. (B) Area Under Curve (AUC) generated from Receiver Operating Characteristic (ROC) curve analysis of RF models with 5, 10, 15, 25, 50 and 100 features. (C) AUC of the 5-feature RF model. (D) Predicted class probabilities (average of the MCCV) for each sample using the best classifiers (based on AUC) of the 5-feature RF model. (E) The average importance of metabolites in the 5-feature RF model based on ROC curve analysis, with the most discriminating feature in descending order of importance. (F) The selected frequencies of metabolites in the 5-feature RF model based on ROC curve analysis.

**Figure 5.** Secondary bioinformatics of annotated metabolites. (A) Topology-based pathway analysis showing metabolic networks in oyster larvae potentially affected by OsHV-1  $\mu$ Var. The most impacted metabolic pathways are specified by the volume and the colour of the spheres (yellow = least relevant; red = most relevant) according to their statistical relevance and pathway impact (PI) values resulting from Quantitative Enrichment Analysis (QTA) and Network Topology Analysis (NTA), respectively. (B–E) Examples of four pathways containing relatively high metabolite coverages: (B) Tricarboxylic acid cycle ( $p < 0.001$ , FDR  $< 0.000$ , PI = 0.26); (C) Alanine, aspartate and glutamate metabolism ( $p < 0.001$ , FDR = 0.002, PI = 0.72); (D) Glutathione metabolism ( $p = 0.057$ , FDR = 0.107, PI = 0.48); (E) Cysteine and methionine metabolism ( $p = 0.033$ , FDR = 0.076, PI = 0.60). Boxes which vary from yellow to red represent metabolites (KEGG ID codes) that were detected and annotated with our methods. Their colour indicates the level of significance (light yellow:  $p > 0.05$ , light orange to red:  $p < 0.05$ ) from unpaired  $t$ -tests (control vs treatment). Light blue boxes/compounds in the pathways were not detected, but were used as background information for QEA to calculate the proportion of identified compounds within each pathway, and in NTA to determine the position (relative-betweenness centrality) and importance of each metabolite.

**Figure 6.** Metabolite–metabolite Pearson correlation heatmaps of healthy control larvae (A) vs. unhealthy virus-exposed larvae (B). The order of metabolites are the same for each of the heatmaps so direct comparisons can be made for particular regions.

**Figure 7.** Correlation Network Analysis of control (A) vs. virus exposed larvae (B). Metabolite–metabolite Pearson correlations > 0.9 are represented by grey solid lines, whereas those that are < 0.9 are represented by dashed grey lines.

**Supplementary Table 1.** List of identified metabolites showing the effect of OsHV-1 infection on oyster larvae. Up and down arrows represent metabolite levels which were identified as being significantly higher or lower in the virus infected group compared to control animals (via t-test, SAM and/or EBAM), or with high (> 1.0) Variable of Importance (VIP) scores in the PLS-DA model.

**Supplementary Table 2.** List of unannotated metabolites showing the effect of OsHV-1 infection on oyster larvae. Up and down arrows represent metabolite levels which were identified as being significantly higher or lower in the virus infected group compared to control animals (via t-test, SAM and/or EBAM), or with high (> 1.0) Variable of Importance (VIP) scores in the PLS-DA model.

**Supplementary Table 3.** List of altered metabolic pathways in larval hosts during viral (OsHV-1  $\mu$ Var) infection.

Figure 1.

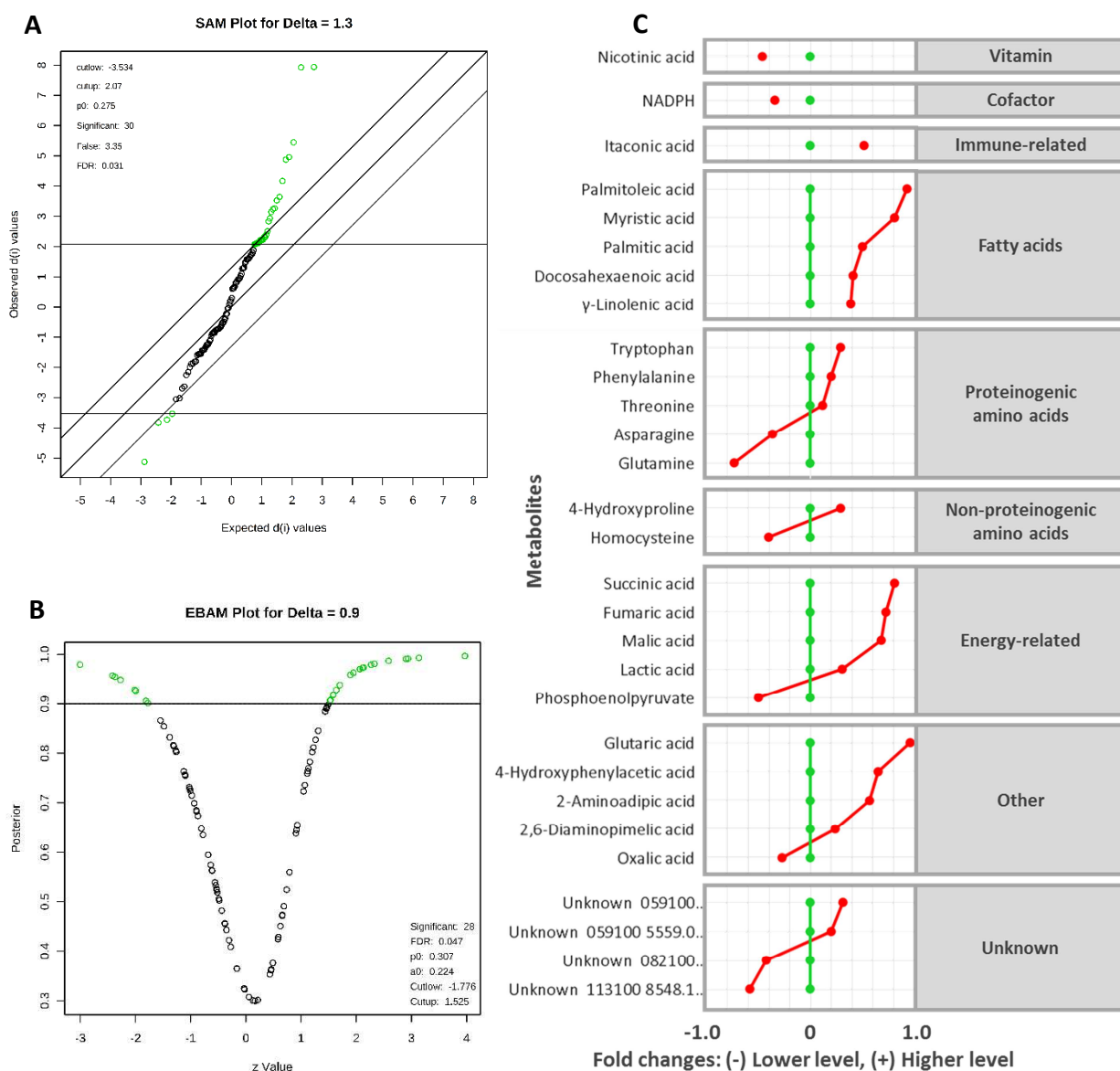


Figure 2.

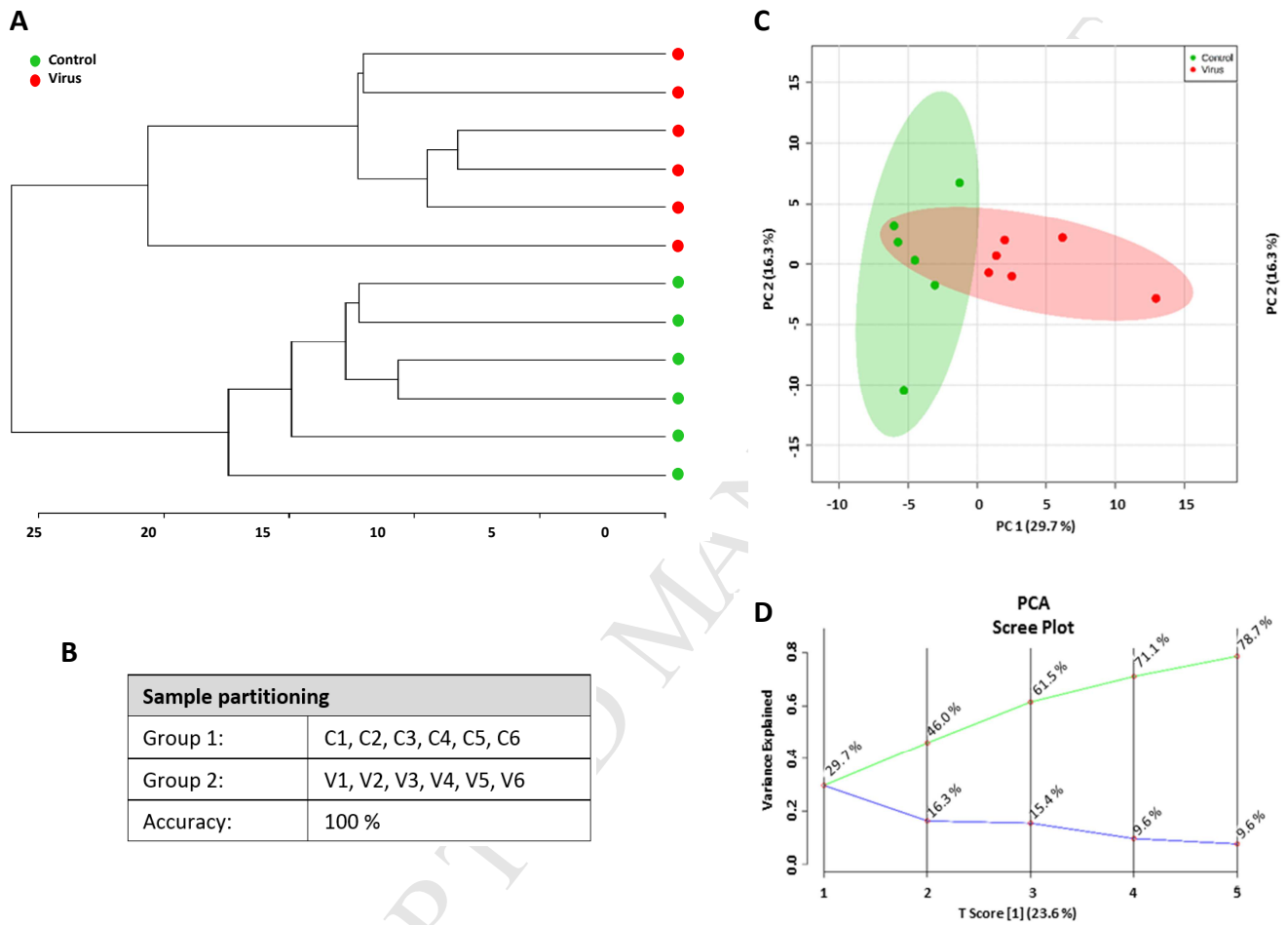


Figure 3.

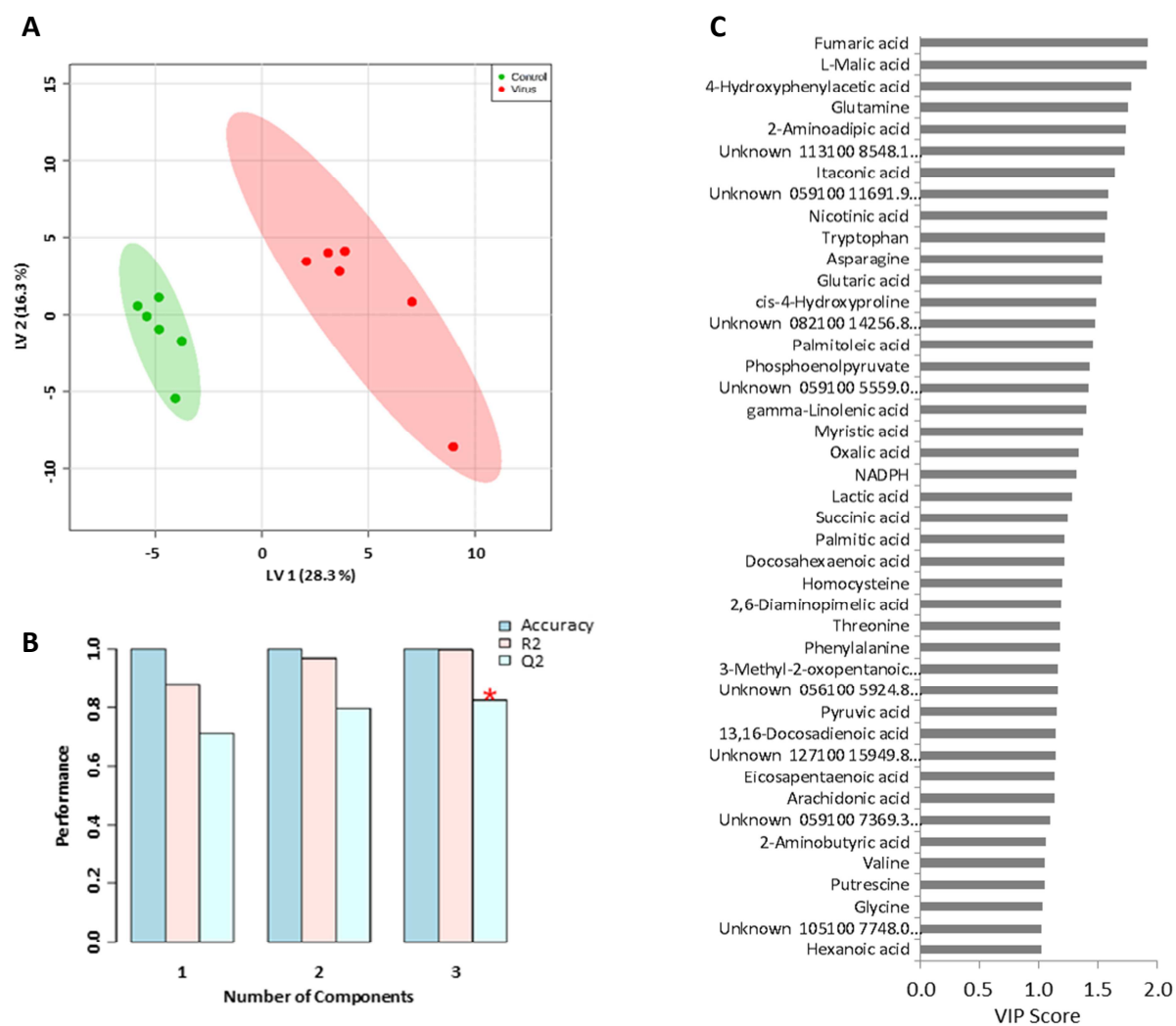
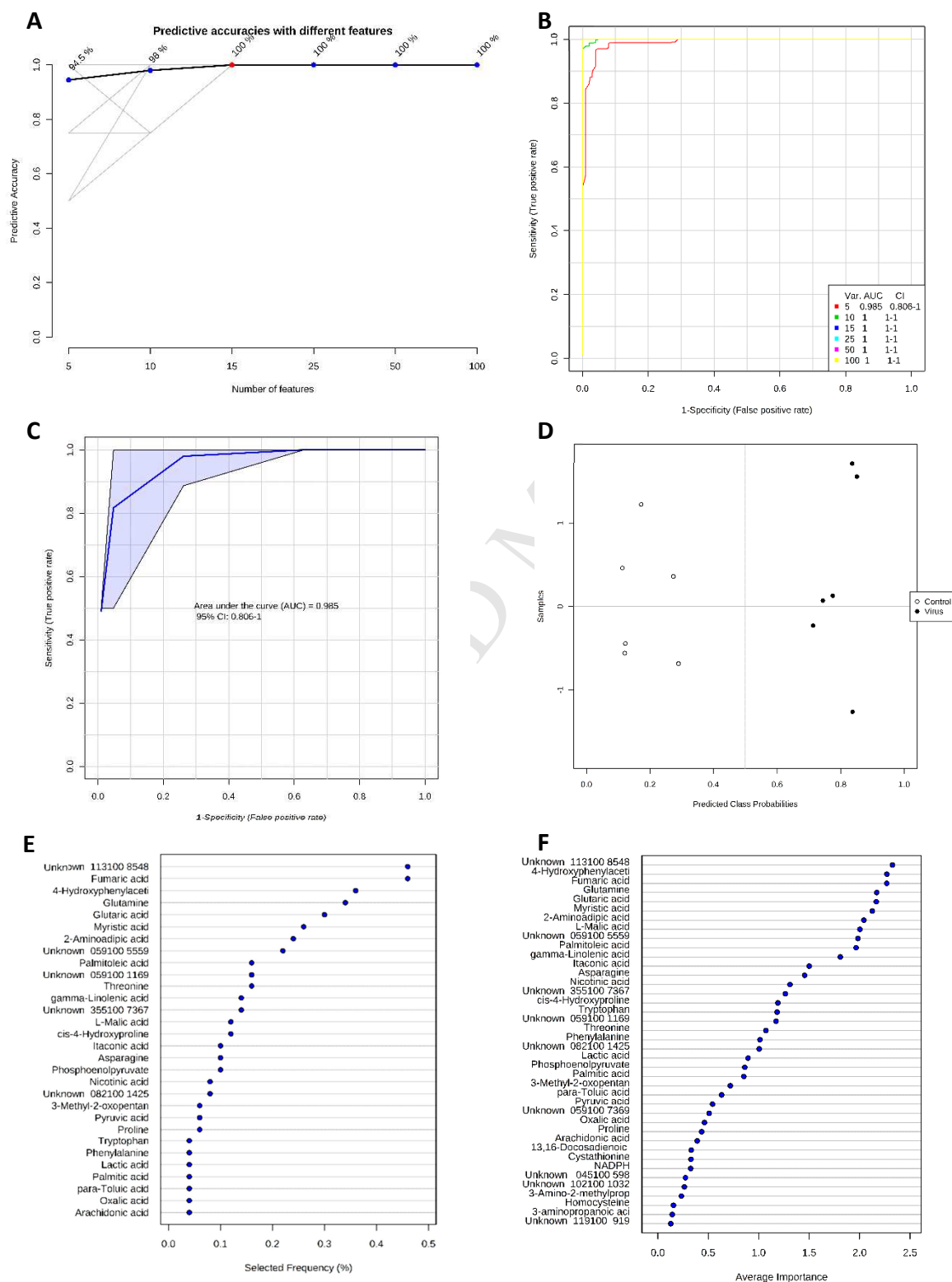


Figure 4.



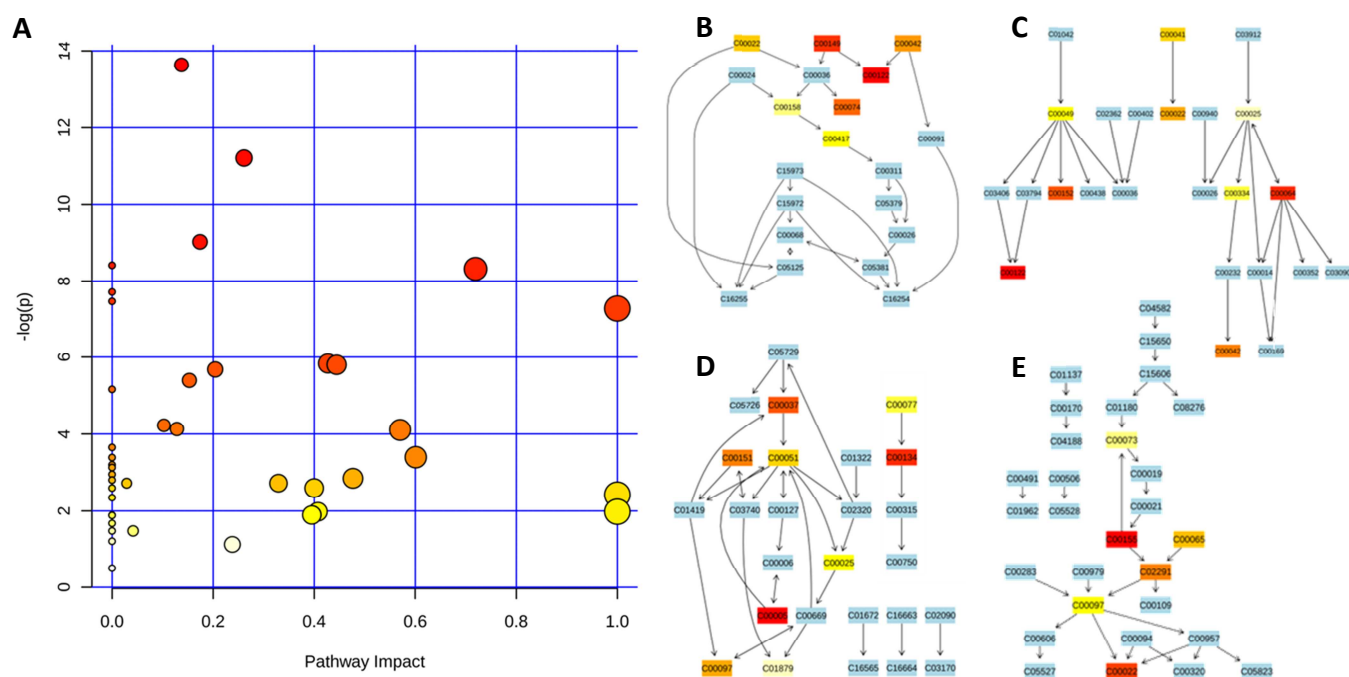
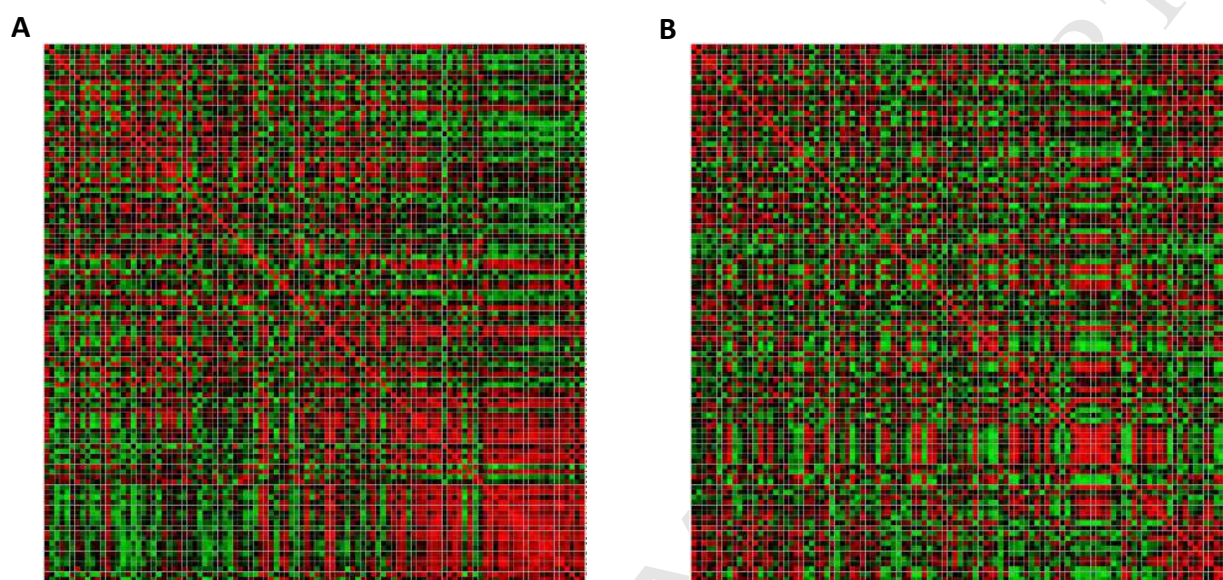
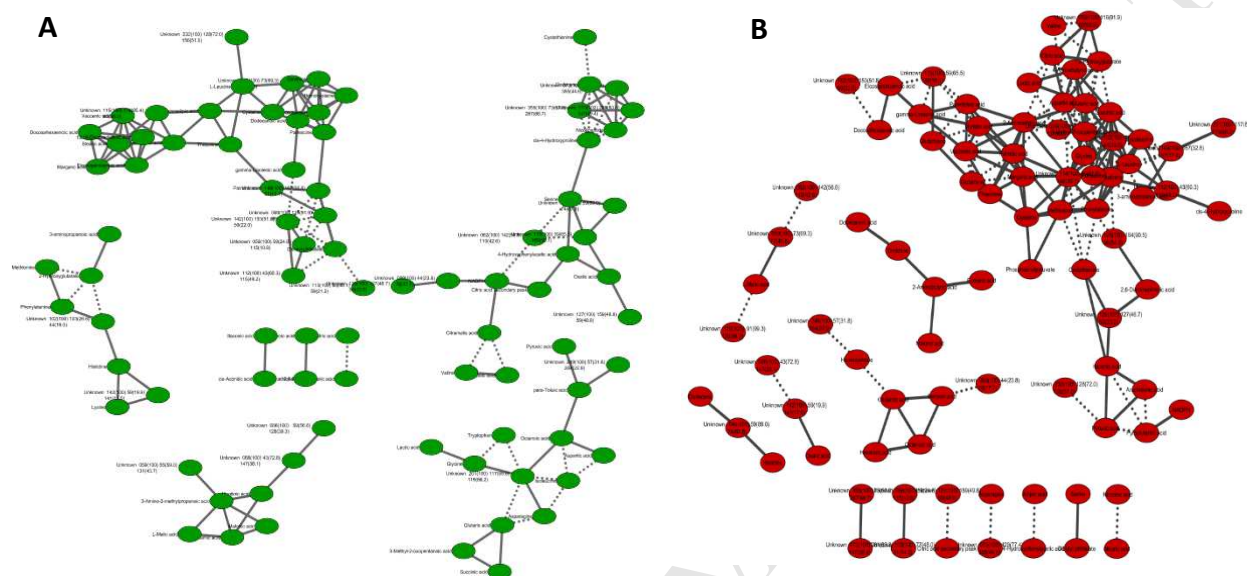




Figure 6.



**Figure 7.**



**HIGHLIGHTS**

- Herpesvirus-induced metabolic responses were investigated in oyster larvae by GC-MS
- Host metabolism changes are suggestive of Irg-1-like activation
- Energy and lipid metabolism was substantially disturbed during infection
- Activation of immunoresponsive gene 1 and the Warburg effect is hypothesised
- Metabolomics is a powerful approach to study disease in early oyster life stage